Contents

Acceptance Probabilities for a Sampling Procedure Based on the Mean and an Order Statistic

Mary C. Croarkin* and Grace L. Yang**

National Bureau of Standards, Washington, DC 20234

A dual acceptance criterion based on the sample mean and an extreme order is used in many inspection procedures. Computation of the acceptance probability for such a dual criterion is investigated. An approximation and a lower bound to the acceptance probability are derived and are applicable to any continuous distribution. In addition, the connection between this dual criterion and hypothesis testing of scale and location parameters is studied. In the case of the exponential distribution the exact evaluation of the acceptance probability yields the power of the test.

Key words: acceptance probability; compliance sampling; dual acceptance criteria; mixed sampling plan; order statistics; statistical methods.

TABLE OF CONTENTS

*Center for Applied Mathematics, National Engineering Laboratory.
**Center for Applied Mathematics, National Engineering Laboratory and the University of Maryland, College Park, MD.

1. Introduction

Suppose that a random sample of size n from a lot is measured with respect to a particular variable and that the acceptance or rejection of the lot depends upon whether or not the measurements satisfy certain criteria. "Lot" can refer to a group of individual items or to a specified amount of material which can be sampled randomly.

There is widespread interest in sampling procedures that specify acceptance criteria involving the sample mean and a proportion of defectives in the sample [1], [4], [5], [9], [11] and [14].[1] Such a sampling procedure might specify that the lot is to be accepted only if the sample mean is greater than a value μ_o, say, and if no more than a specified percentage of the sample is less than a lower limit L. The purpose of a dual acceptance criterion is to ensure, for example, that the lot is at least a stated amount, μ_0, of the specified variable on the average and that the number of so called "defectives" or items that violate the lower limit is controlled. Obviously, depending on the application, the acceptance criteria can be specified in the opposite direction; i.e., the lot is to be accepted only if the sample mean is less than μ_0 and at least a certain percentage of the sample is greater than an upper limit U.

Specifically, let $X_1, \cdots, X_n$ be a random sample of n measurements, and let $X_{(1)} \leqslant \cdots \leqslant X_{(n)}$ be the corresponding order statistics. It is assumed that the random variables $X_1, \cdots, X_n$ are independent and identically distributed (i.i.d.) with a probability density function $f(x)$, and that the X_j have finite mean μ and variance o^2. Let $\overline{X}$ be the sample mean and N_L be the number of defectives or measurements having values smaller than the specified (lower) limit L.

The sampling procedure to be considered is such that the lot is accepted whenever

$$[\overline{X} \geqslant \mu_0 \text{ and } N_L \leqslant k] \tag{1.1}$$

where μ_0 and k are specified in the sampling plan.

In terms of the order statistics, (1.1) is equivalent to the criterion

$$[\overline{X} \geqslant \mu_0 \text{ and } X_{(k+1)} > L] \tag{1.2}$$

and the probability of accepting the lot is defined to be

$$P_n = P[\overline{X} \geqslant \mu_0, N_L \leqslant k]. \tag{1.3}$$

The sampling procedure discussed above is a mixed variables-attributes acceptance criterion based on one sample. There are various ways of designing a mixed sampling plan. The type studied by Schilling and Dodge [19] is a double sampling procedure involving variables inspection in the first sample. If the variables inspection does not lead to acceptance, a second sample is taken and an attribute inspection is conducted on the combined samples. In their work, Schilling and Dodge assume a normal distribution with unknown mean and known variance.

We concentrate on a single sample plan where both the variables inspection as specified by the sample mean and attributes inspection as specified by k, the number of allowable defectives, are conducted on the same sample. This causes difficulties in the computation of the acceptance probabilities because of the lack of independence of the sample mean and the order statistics.

Investigations, of which we are aware, into the statistical properties of sampling procedures of this type assume a normal distribution with unknown mean and known variance. For instance in a compliance sampling application, Weed [21] simulates a two-stage procedure used in specifications for the thickness of paving material in which both stages involve a variable and an attribute inspection. Elder and Muse [8] develop a large sample approximation for the acceptance probability used in U.S. Department of Agriculture inspection procedures (1.3) and compare the approximation to an exact numerical procedure.

---

[1]Figures in brackets indicate literature references at the end of this paper.

It is noted that the dual sampling criterion leads to an acceptance region for testing hypotheses concerning the mean μ and the probability of item defectiveness simultaneously. The probability of a defective is defined to be $p = P[X \leqslant L]$. The acceptance region in (1.1) or (1.2) may be used for testing the null hypothesis

$$H_0: \mu = \mu^* \text{ and } p = p^*$$

versus the alternatives   (1.4)

$$H_1: \mu < \mu^* \text{ or } p > p^*$$

Through reparametrization, these hypotheses may be formulated in terms of the location and scale parameters. Evidently, this depends on the properties of the distribution under consideration.

In the case of the normal distribution $N(\mu, \sigma^2)$, the probability of a defective is

$$p = \Phi\left(\frac{L - \mu}{\sigma}\right)$$ (1.5)

where

$$\Phi(z) = \frac{1}{\sqrt{2\pi}} \int_{-\infty}^{z} \exp\{-u^2/2\} du.$$

Thus,

$$\sigma = (L - \mu)/\Phi^{-1}(p).$$ (1.6)

Consequently, $\mu = \mu^*$ and $p = p^*$ if and only if

$$\mu = \mu^* \text{ and } \sigma = \sigma^* = (L - \mu^*)/\Phi^{-1}(p^*).$$

Accordingly, the hypothesis testing problem in (1.4) becomes that of testing

$$H_0: \mu = \mu^* \text{ and } \sigma = \sigma^*$$

versus   (1.7)

$$H_1: \mu < \mu^* \text{ or } \sigma < \frac{L - \mu}{\Phi^{-1}(p^*)}.$$

Perusal of the literature turned up very few papers that are directly related to a joint test of the location and scale parameters. Eisenberger [7] develops an asymptotic joint test for the mean and variance of a normal distribution based on a quantile. Perng [18] develops a joint test for the location and scale parameters of an exponential distribution based on Fisher's method of combining two test statistics. Anderson [2] discusses the likelihood ratio test for simultaneously testing the mean and variance in multivariate normal distributions; both one-sample and k-sample problems are considered. In a recent paper, Perlman [17] shows that the likelihood ratio test is unbiased. None of these papers discusses the computation of acceptance probabilities under alternative hypotheses. Also, unlike (1.7), the alternatives in the quoted papers are rectangular regions.

2. Scope of the Study

It is our intention to investigate the acceptance probability of a dual sampling procedure from several aspects. The investigations are carried out for the normal distribution because of its im-

portance in acceptance sampling and for the exponential and Weibull distributions because of their application in modeling the life span distribution.

First, in section 3, we derive a large sample approximation P_a for the acceptance probability P_n. This is achieved by deriving the asymptotic joint distribution of $\sqrt{n}(\overline{X}-\mu)/\sigma$ and $(N_L-np)/(np(1-p))^{1/2}$ as the sample size approaches infinity. This approximation method applies to any distribution. We illustrate its use in the normal, Weibull, and exponential distributions. The results as given in sections 3.1, 3.2, and 3.3 are compared with a simulation study.

In section 4 a lower bound $\underline{P}$ is established for P_n that amounts to assuming the independence of the sample mean and the kth order statistic. This lower bound for finite samples provides some information on the accuracy of the approximation. We attempt to determine under what conditions the approximation P_a is a significant improvement over the lower bound. In this connection one notes that a large sample approximation P_a is derived by normalizing the sample mean as $\sqrt{n}(\overline{X}-\mu)/\sigma$ and the number of defectives in the sample as $(N_L-np)/(np(1-p))^{1/2}$. If, instead, we convert N_L to an order statistic $X_{(k)}$ and consider $X_{(k)}$ (or $X_{(n-k)}$) as an extreme statistic, the normalized sample mean $\sqrt{n}(\overline{X}-\mu)$ and $X_{(k)}$ (or equivalently $X_{(n-k)}$) are asymptotically independent (The proof is given in appendix B). This suggests that $\underline{P}$ serves as a possible approximation to P_n when n is large and k is small.

In other words, when comparing P_a and $\underline{P}$, one should keep in mind the relationship between k and n; namely, the ratio k/n. In the case of P_a we have $N_L/n \to p$ and in the case of an extreme statistic we have $k/n \to 0$ as $n \to \infty$. Clearly, one would expect that the lower bound $\underline{P}$ may be a reasonable approximation when k is relatively small compared with n. This is indeed confirmed in our numerical study in section 4. The numerical studies show that P_a is comparable to $\underline{P}$ for small k/n and superior to $\underline{P}$ for larger values of k/n.

Finally, in section 5 the acceptance probabilities are approximated for the normal and Weibull distributions using a procedure proposed by Pearson and Hartley [16]. The exact acceptance probabilities curves are computed for the exponential distribution.

3. Large Sample Approximation of the Joint Distribution of $\overline{X}$ and N_L.

3.1 Derivation

Let $X_1, \cdots, X_n$ be a random sample from the lot with pdf $f(x)$. Assume that X_j has a finite mean μ and variance σ^2.
Introducing indicator random variables I_j,
where

$$I_j = \begin{cases} 1 & \text{if } X_j \leqslant L \\ 0 & \text{if } X_j > L \end{cases} \tag{3.1.1}$$

and letting the probability that an item violates the lower specification limit L be

$$p = P[X_j \leqslant L], \tag{3.1.2}$$

we can write the number of (unit) lower limit violations N_L in the sample as

$$N_L = \sum_{j=1}^{n} I_j. \tag{3.1.3}$$

Note that N_L has a binominal distribution $B(n,p)$, and the event $[N_L \leqslant k]$ is equivalent to the event $[X_{(k+1)} > L]$. In order to develop an approximation formula for the acceptance probability

$$P_n = P[\overline{X} \geqslant \mu_0, N_L \leqslant k],$$

we consider random variables W_n and Y_n defined as

$$\begin{aligned} W_n &= n^{1/2}(\overline{X}-\mu)/\sigma \\ \text{and} \\ Y_n &= (N_L-np)/(np(1-p))^{1/2}. \end{aligned} \tag{3.1.4}$$

Let (W_n, Y_n) be a row vector. We prove the following result.

THEOREM 3.1. *As* $n \to \infty$, *the random vector* $(W_n, Y_n)'$ *converges in distribution to a bivariate normal distribution with mean $(0,0)'$ and covariance matrix*

$$\Sigma = \begin{pmatrix} 1 & \varrho \\ \varrho & 1 \end{pmatrix} \tag{3.1.5}$$

where

$$\varrho = E\ (X_j-\mu)I_j/\sigma(p(1-p))^{1/2}. \tag{3.1.6}$$

PROOF: Let t_1 and t_2 be arbitrarily chosen but fixed real numbers. Form the linear combination of W_n and Y_n, $t_1 W_n + t_2 Y_n$.

Direct computation and application of the central limit theorem give

$$t_1 W_n + t_2 Y_n \quad \overset{D}{\to} \quad N\ (0,\ t_1{}^2 + t_2{}^2 + t_1t_2\varrho)\ \text{as}\ n \to \infty$$

It then follows from application of the Cramer-Wold device that

$$\begin{pmatrix} W_n \\ Y_n \end{pmatrix} \quad \overset{D}{\to} \quad N\left(\begin{pmatrix} 0 \\ 0 \end{pmatrix},\ \Sigma \right) \text{as}\ n \to \infty$$

where Σ is given in (3.1.5).

Making use of the asymptotic distribution in Theorem 3.1, we note from (3.1.4) that

$$\overline{X} = n^{-1/2}\sigma W_n + \mu$$

and

$$N_L = (np(1-p))^{1/2} Y_n + np.$$

Thus the random vector $(\overline{X}, N_L)'$ has asymptotically a bivariate normal distribution with mean and covariance matrix Γ given by

$$\begin{pmatrix} \mu \\ np \end{pmatrix} \text{and } \Gamma = \begin{pmatrix} \dfrac{\sigma^2}{n} & E(X_j-\mu)I_j \\ E(X_j-\mu)I_j & np(1-p) \end{pmatrix} \tag{3.1.7}$$

respectively.

For convenience in computation, write the acceptance probability P_n as

$$P_n = P[\overline{X} \geqslant \mu_0] - P[\overline{X} \geqslant \mu_0, N_L > k]$$

$$= P[\overline{X} \geqslant \mu_0] - P[W_n \geqslant \sqrt{n}(\mu_0-\mu)/\sigma,\ Y_n > (np(1-p))^{-1/2}(k-np)]. \tag{3.1.8}$$

Making use of (3.1.7) and the continuity correction factor 0.5 for the random variable N_L, we see that for sufficiently large n, P_n may be approximated by

$$P_a = \frac{1}{\sqrt{2\pi}} \int_a^\infty \exp(-z^2/2)dz - \int_a^\infty \int_b^\infty g(x,y,\varrho)dxdy \qquad (3.1.9)$$

where

$$a = \sqrt{n}(\mu_0-\mu)/\sigma, \qquad (3.1.10)$$

$$b = (np(1-p))^{-1/2}(k + 0.5 - np), \qquad (3.1.11)$$

$$g(x,y,\varrho) = (2\pi)^{-1}(1-\varrho^2)^{-1/2}\exp\{-(x^2 + y^2 - 2\varrho xy)/2(1-\varrho^2)\}, \qquad (3.1.12)$$

and ϱ is defined in (3.1.6).

In order to compute the $P[\overline{X} \geqslant \mu_0, N_L \leqslant k]$ using the approximation P_a, we need to know the mean μ and the variance σ^2 of the distribution in question, the proportion defective p as defined in (3.1.2) and the correlation coefficient ϱ as defined in (3.1.6). The computation of the bivariate normal term is described in more detail in Appendix A.

3.2 Normal Distribution

Assume that the sample comes from a normal distribution $N(\mu,\sigma^2)$.
The item defective probability from (3.1.2) is

$$p = P[X \leqslant L] = \Phi\{(L-\mu)/\sigma\}, \qquad (3.2.1)$$

where $\Phi\{(L-\mu)/\sigma\}$ is the cdf of the $N(0,1)$ given in (1.5).

In order to compute the approximation P_a given in (3.1.9), we need to compute the correlation coefficient given in (3.1.6).

The expectation $E\{(X-\mu)I_{[X\leqslant L]}\}$ is evaluated as

$$E\{(X-\mu)I_{[X\leqslant L]}\} = -\frac{\sigma}{\sqrt{2\pi}}\exp\{-(L-\mu)^2/2\sigma^2\}.$$

Consequently the correlation coefficient is

$$\varrho = -(2\pi p(1-p))^{-1/2}\exp\{-(L-\mu)^2/2\sigma^2\}.$$

In order to compare the approximation P_a in (3.1.9) with an approximation developed by Elder and Muse [8], the lower limit L is chosen under the assumption that $\mu = 0$, $\sigma = 1$, and according to the criterion

$$P[N_L \leqslant k] = 1-\alpha, \qquad (3.2.2)$$

where $0 < \alpha < 1$.

Because N_L is $B(n,p)$, the lower limit L is determined from

$$\sum_{j=0}^k \binom{n}{j} p^j(1-p)^{n-j} = 1-\alpha, \qquad (3.2.3)$$

where $p = \Phi(L)$.

Values of L as tabulated by Elder and Muse for $\alpha = 0.10$, 0.05, and 0.01 are shown in table I. Once

		Lower Limit L		
n	k	$\alpha = 0.10$	$\alpha = 0.05$	$\alpha = 0.01$
5	0	2.036	2.319	2.877
	1	1.215	1.429	1.843
	2	0.685	0.881	1.250
10	0	2.309	2.568	3.089
	1	1.602	1.789	2.157
	2	1.196	1.358	1.670
20	0	2.559	2.799	3.289
	1	1.928	2.095	2.428
	2	1.586	1.726	2.001
30	0	2.696	2.928	3.402
	1	2.100	2.258	2.574
	2	1.783	1.914	2.172

L is determined the correlation coefficient of $\overline{X}$ and N_L can be evaluated as

$$\varrho = -[2\pi p(1-p)]^{-1/2} \exp\{-L^2/2\}. \tag{3.2.4}$$

The Elder-Muse approximation along with their exact results are compared with the corresponding values of P_a in table II where L is chosen such that $\alpha = 0.10$.

The comparison with the exact values derived in [8] shows that even for small sample size P_a provides an excellent approximation to the acceptance probability P_n, and its effectiveness increases as k gets larger. When $k = 0$, the percent error in P_a as compared to the exact results is approximately 3 percent. For $k = 1$, it is about 1 percent and for $k = 2$, it is less than 1 percent. The percentage errors in both P_a and the Elder-Muse approximation when $\mu = 0$ are shown below.

	Percent Error in Approximations					
	$k = 0$		$k = 1$		$k = 2$	
n	P_a	Elder Muse	P_a	Elder Muse	P_a	Elder Muse
5	3.3	1.0	1.0	1.8	0.6	1.2
10	3.1	0.6	1.0	1.0	0.6	1.2
20	3.0	0.2	0.8	0.6	0.6	0.8
30	2.6	0.2	0.8	0.8	0.4	0.6

3.3 Weibull Distribution

Assume that the sample $X_1,...,X_n$ comes from a two parameter Weibull distribution $W(\lambda,\theta)$ with scale parameter λ, shape parameter θ and *pdf*

$$f(x) = (\theta/\lambda) \ (x/\lambda)^{\theta-1} \exp\{-(x/\lambda)^\theta\} \ \text{for } x > 0, \lambda > 0, \theta > 0 \tag{3.3.1}$$

The mean and variance are

$$\mu = \lambda\Gamma(1+1/\theta) \tag{3.3.2}$$

and

$$\sigma^2 = \lambda^2 \{\Gamma(1+2/\theta) - [\Gamma(1+1/\theta)]^2\} \tag{3.3.3}$$

respectively where $\Gamma(\cdot)$ is the gamma function.

For $0 < \theta \leqslant 1$, X has a decreasing failure rate (DFR) distribution; for $\theta \geqslant 1$, X has an increasing failure rate (IFR) distribution. For further information see Johnson and Kotz [13].

In the case of the Weibull distribution, the proportion defective p is defined from (3.1.2) and (3.2.2) as

$$p = [X \leqslant L] = 1 - \exp\{-(L/\lambda)^\theta\}. \tag{3.3.4}$$

The expectation

$$EXI_{[X \leqslant L]} = \frac{\theta}{\lambda} \int_0^L x(x/\lambda)^{\theta-1}\exp\{-(x/\lambda)^\theta\}dx$$

$$= \lambda\, I\{(L/\lambda)^\theta, 1/\theta\} \tag{3.3.5}$$

and $I(c,d)$ is related to the incomplete Γ-function [12].

Combining (3.1.6), (3.3.4) and (3.3.5), we find that the correlation coefficient is

TABLE II. *Comparison of Approximation* P_a *with*
Elder —Muse Values for
$P[X \geqslant \mu_o{}^*, N_L \leqslant k]$ *where* $P(N_L \leqslant k) = 0.90$
for Normal Distribution N(0,1)

		k=0			k=1			k=2		
n	μ	Exact	P_a	Elder Muse	Exact	P_a	Elder Muse	Exact	P_a	Elder Muse
5	−.8	0.035	0.034	0.032	0.036	0.036	0.034	0.037	0.036	0.037
	−.6	0.087	0.082	0.085	0.089	0.088	0.089	0.089	0.089	0.091
	−.4	0.180	0.168	0.181	0.184	0.181	0.188	0.185	0.184	0.189
	−.2	0.318	0.300	0.323	0.324	0.320	0.332	0.326	0.325	0.333
	.0	0.488	0.472	0.493	0.496	0.491	0.505	0.499	0.496	0.505
	.2	0.659	0.667	0.663	0.669	0.672	0.674	0.671	0.672	0.674
	.4	0.801	0.814	0.802	0.811	0.814	0.811	0.813	0.814	0.812
	.6	0.899	0.910	0.899	0.908	0.910	0.906	0.909	0.910	0.906
	.8	0.956	0.963	0.955	0.962	0.963	0.959	0.963	0.963	0.959
10	−.6	0.027	0.026	0.026	0.028	0.028	0.026	0.028	0.028	0.027
	−.4	0.098	0.091	0.097	0.100	0.098	0.099	0.101	0.101	0.101
	−.2	0.252	0.236	0.253	0.257	0.252	0.261	0.260	0.257	0.264
	.0	0.480	0.465	0.483	0.490	0.485	0.495	0.494	0.491	0.500
	.2	0.713	0.732	0.714	0.725	0.735	0.728	0.731	0.736	0.733
	.4	0.876	0.897	0.876	0.888	0.897	0.887	0.893	0.897	0.891
	.6	0.956	0.971	0.956	0.966	0.971	0.965	0.969	0.971	0.967
	.8	0.956	0.994	0.985	0.992	0.994	0.991	0.993	0.994	0.993
20	−.4	0.034	.0.032	0.034	0.035	0.034	0.034	0.036	0.035	0.034
	−.2	0.174	0.162	0.174	0.178	0.173	0.178	0.180	0.177	0.181
	.0	0.474	0.460	0.475	0.483	0.479	0.486	0.488	0.485	0.492
	.2	0.781	0.811	0.781	0.795	0.814	0.795	0.802	0.814	0.802
	.4	0.937	0.963	0.937	0.950	0.963	0.950	0.956	0.963	0.955
	.6	0.981	0.996	0.981	0.991	0.996	0.991	0.994	0.996	0.993
30	−.4	0.013	0.012	0.013	0.013	0.013	0.013	0.014	0.014	0.013
	−.2	0.127	0.118	0.127	0.130	0.126	0.129	0.131	0.129	0.131
	.0	0.470	0.458	0.471	0.479	0.476	0.480	0.484	0.482	0.487
	.2	0.824	0.861	0.824	0.839	0.863	0.839	0.847	0.863	0.846
	.4	0.958	0.986	0.958	0.972	0.986	0.972	0.978	0.986	0.977
	.6	0.985	0.999	0.985	0.995	0.999	0.995	0.997	0.999	0.997

*$\mu_0 = 0$

492

$$\varrho = [\lambda I\{(L/\lambda)^\theta, 1/\theta\} - \mu p]/\sigma(p(1-p))^{1/2} \qquad (3.3.6)$$

where μ and σ are defined by (3.3.2), and (3.3.3) respectively.

The limits of integration for the approximation (3.1.9) are

$$a = \frac{n^{1/2}[\mu_0 - \lambda\Gamma(1 + 1/\theta)]}{\lambda\{\Gamma(1 + 2/\theta) - [\Gamma(1 + 1/\theta)]^2\}^{1/2}} \qquad (3.3.7)$$

and b as defined in (3.1.11).

As is the case in the normal distribution, the lower limit L is determined according to (3.2.3) and (3.3.4) for specified values of k and α.

Explicitly

$$L = \lambda\,[-\log_e(1-p)]^{1/\theta}. \qquad (3.3.8)$$

The proportion defective p is tabulated in table III for $\alpha = 0.10$, 0.05 and 0.01, $n = 5, 10, 20, 30$ and $k = 0, 1, 2, 3$. Corresponding lower limits L where $\lambda = 1$ are shown in table IV.

TABLE III. *Proportion Defectives p used in Computation of Acceptance Probabilities*

| n | k | Proportion Defective p | | |
		$\alpha = 0.10$	$\alpha = 0.05$	$\alpha = 0.01$
5	0	0.0208	0.0102	0.00200
	1	.112	.0765	.0330
	2	.247	.1890	.106
	3	.416	.3425	.222
10	0	0.0105	0.00511	0.00100
	1	.0545	.0365	.0155
	2	.1155	.0870	.0475
	3	.1875	.1500	.0930
20	0	0.00525	0.00256	0.000500
	1	.0269	.0180	.00759
	2	.0564	.0422	.0227
	3	.0902	.0713	.0435
30	0	0.00350	0.00171	0.000335
	1	.0178	.0120	.00500
	2	.0373	.0278	.0149
	3	.0594	.0468	.0285

The approximation P_a is compared to a simulation study where the acceptance probability was computed from 5,000 random samples. Simulation for the Weibull distribution was done by generating independent uniform random deviates U_i using a congruential random number generator and making the transformation

$$X_i = \lambda(-\log_e U_i)^{1/\theta}$$

The X_i are independent $W(\lambda, \theta)$ r.v.s with pdf as shown in (3.3.1).

Values of P_a and simulated acceptance probabilities are tabulated in table V for Weibull distribution $W(1, \theta)$ for $\theta = 1, 2, 3.5$.

The accuracy of the approximation P_a as gauged by the simulation results is dependent on several factors; i.e., namely, the value of the shape parameter θ; α, the probability that the sample will contain more than the allowable number of defectives; n, the size of the sample; and k, the number of allowable defectives or number of measurements less than the lower limit L.

The worst accuracy is for a Weibull distribution with $\theta = 1$ where α is small, $\alpha = 0.01$, and n is small, $n = 5$. The error is 9 percent for this case but drops to 2 percent when the sample size is in-

TABLE IV. *Lower Limits Used in Computation of Acceptance Probabilities for Weibull Distribution*

	n	k	Lower Limit L		
			$\alpha=0.10$	$\alpha=0.05$	$\alpha=0.01$
$\theta=1$	5	0	0.0210	0.0103	0.0020
	5	1	.1188	.0796	.0336
	5	2	.2837	.2095	.1120
	5	3	.5379	.4193	.2510
	10	0	.0106	.0051	.0010
	10	1	.0560	.0372	.0156
	10	2	.1227	.0910	.0487
	10	3	.2076	.1625	.0976
	20	0	.0053	.0026	.0005
	20	1	.0273	.0182	.0076
	20	2	.0581	.0431	.0230
	20	3	.0945	.0740	.0445
	30	0	.0035	.0017	.0003
	30	1	.0180	.0121	.0050
	30	2	.0380	.0282	.0150
	30	3	.0612	.0479	.0289
$\theta=2$	5	0	.1450	.1013	.0447
	5	1	.3446	.2821	.1832
	5	2	.5326	.4577	.3347
	5	3	.7334	.6475	.5010
	10	0	.1027	.0716	.0316
	10	1	.2367	.1928	.1250
	10	2	.3503	.3017	.2206
	10	3	.4557	.4031	.3124
	20	0	.0726	.0506	.0224
	20	1	.1651	.1348	.0873
	20	2	.2409	.2076	.1515
	20	3	.3075	.2720	.2109
	30	0	.0592	.0414	.0183
	30	1	.1340	.1099	.0708
	30	2	.1950	.1679	.1225
	30	3	.2475	.2189	.1700
$\theta=3.5$	5	0	.3317	.2702	.1694
	5	1	.5441	.4852	.3791
	5	2	.6977	.6398	.5351
	5	3	.8376	.7801	.6737
	10	0	.2724	.2216	.1390
	10	1	.4390	.3904	.3047
	10	2	.5492	.5042	.4216
	10	3	.6382	.5950	.5144
	20	0	.2233	.1818	.1140
	20	1	.3573	.3181	.2482
	20	2	.4434	.4073	.3402
	20	3	.5097	.4752	.4109
	30	0	.1988	.1620	.1017
	30	1	.3171	.2831	.2202
	30	2	.3929	.3607	.3013
	30	3	.4502	.4198	.3633

TABLE V. *Comparison of Approximation P_a with Simulation for*
$P(\overline{X} \geqslant \mu_0^*, N_L \leqslant k)$ *where* $P(N_L \leqslant k) = 1 - \alpha$
for Weibull Distribution $W(1, \theta)$.

	n	k	Probability of Acceptance					
			$\alpha = 0.10$		$\alpha = 0.05$		$\alpha = 0.01$	
			P_a	Simul	P_a	Simul	P_a	Simul
$\theta = 1$	5	0	0.645	0.634	0.698	0.663	0.712	0.672
	5	1	.668	.652	.698	.673	.712	.672
	5	2	.678	.664	.699	.680	.711	.674
	5	3	.688	.674	.702	.684	.711	.675
	10	0	.705	.707	.768	.755	.785	.773
	10	1	.726	.724	.768	.763	.785	.776
	10	2	.733	.734	.766	.768	.785	.778
	10	3	.738	.743	.767	.772	.784	.779
	20	0	.775	.795	.848	.828	.868	.875
	20	1	.795	.801	.846	.836	.868	.877
	20	2	.798	.807	.844	.840	.867	.879
	20	3	.801	.810	.843	.841	.867	.878
	30	0	.815	.826	.893	.872	.914	.914
	30	1	.835	.837	.890	.879	.914	.918
	30	2	.837	.838	.887	.878	.914	.915
	30	3	.838	.841	.886	.881	.913	.917
$\theta = 2$	5	0	.681	.703	.720	.731	.744	.738
	5	1	.709	.723	.729	.734	.744	.739
	5	2	.721	.736	.733	.737	.744	.740
	5	3	.729	.740	.736	.739	.744	.740
	10	0	.743	.764	.788	.807	.824	.822
	10	1	.768	.780	.803	.808	.824	.825
	10	2	.777	.794	.808	.808	.823	.826
	10	3	.784	.800	.812	.810	.823	.827
	20	0	.810	.827	.865	.885	.906	.903
	20	1	.832	.839	.876	.884	.906	.905
	20	2	.837	.848	.884	.882	.905	.907
	20	3	.840	.851	.884	.882	.905	.907
	30	0	.844	.860	.897	.924	.946	.947
	30	1	.865	.866	.903	.922	.946	.950
	30	2	.867	.867	.909	.919	.946	.949
	30	3	.869	.872	.914	.918	.945	.952
$\theta = 3.5$	5	0	.801	.829	.864	.859	.880	.872
	5	1	.830	.844	.865	.873	.880	.875
	5	2	.839	.855	.868	.875	.880	.876
	5	3	.843	.853	.869	.878	.879	.877
	10	0	.853	.864	.931	.911	.951	.942
	10	1	.877	.868	.930	.915	.951	.947
	10	2	.882	.884	.928	.922	.951	.946
	10	3	.885	.889	.928	.925	.951	.950
	20	0	.882	.890	.968	.938	.990	.983
	20	1	.902	.894	.964	.946	.990	.984
	20	2	.903	.899	.960	.946	.990	.987
	20	3	.903	.894	.958	.947	.989	.986
	30	0	.887	.893	.974	.938	.998	.984
	30	1	.908	.896	.970	.947	.998	.989
	30	2	.907	.894	.966	.948	.997	.990
	30	3	.907	.898	.964	.956	.996	.990

$^*\mu_0 = 0.75$

creased to $n = 10$. For other Weibull distributions and combinations of α and n, the worst accuracies occur when $k = 0$, and in this case the errors are as large as 6 percent for $n = 5$ and 4 percent for $n = 30$. However, the approximation P_a works very well when $k > 0$. The disagreement between P_a and the simulation is less than 1 percent for a large proportion of the points when $k > 0$.

3.4 Exponential Distribution

Assume that the sample $X_1,...,X_n$ comes from an exponential distribution $E(\lambda,\beta)$ with location parameter β and scale parameter λ and pdf

$$f(x) = (1/\lambda) \exp \{-(x-\beta)/\lambda\} \qquad x > \beta, \lambda > 0 \tag{3.4.1}$$

The mean and variance of X are given by $\mu = \lambda + \beta$ and $\sigma^2 = \lambda^2$ respectively.
We have

$$p = 1-\exp(-(L-\beta)/\lambda) \tag{3.4.2}$$

and

$$EXI_{[X \leqslant L]} = \lambda p - (1-p)(L-\beta) + \beta p. \tag{3.4.3}$$

Combining (3.4.2) and (3.4.3), we get

$$\varrho = -(1-p)^{1/2}(L-\beta)/\lambda p^{1/2}. \tag{3.4.4}$$

Using values for the proportion defective p that are given in table III, the corresponding limits L as determined by

$$L = \beta - \lambda \log (1-p) \tag{3.4.5}$$

are found in table VI for $\beta = 0$ and $\lambda = 0.5, 1, 2$.
The values a and b appearing in the approximation P_a (3.1.9) are given by

$$a = n^{1/2}\lambda^{-1} (\mu_0-\lambda-\beta) \tag{3.4.6}$$

$$b = (np(1-p))^{-1/2} (k + 0.5 -np)$$

and ϱ is defined by (3.4.4.)
Values of P_a and simulated acceptance probabilities are tabulated in table VII for the exponential distribution $E(\lambda,0)$ for $\lambda = 0.5,1,2$.
The accuracy of the approximation P_a is more dependent on n, the sample size and less dependent on k, the number of allowable defectives for the exponential distribution than for Weibull distributions. The worst accuracy·is for an exponential distribution with $\lambda = 1$, where $k = 0$ and $n = 5$. The disagreement with the simulation in this case is 7 percent, dropping to 1 percent when the sample size is increased to $n = 10$. In general, the accuracies are not dependent upon the parameter λ but are somewhat dependent upon the way in which the lower limit L is chosen, and the accuracies tend to worsen as the probability of the sample containing more than the allowable number of defectives increases. Accuracies of about 2 percent are characteristic of the results over all values of k.

4. A Lower Bound for the Acceptance Probability

A lower bound for the acceptance probability is provided by the following lemma.

LEMMA 4.1: *Let* $X_1,...,X_n$ *be i.i.d random variables from a continuous distribution. Let* $\overline{X}$ *be the*

sample mean and $X_{(r)}$ *be the* r^{th} *smallest order statistic of* $X_1,...,X_n$ *. Then for arbitrarily fixed real numbers* a, b *and positive integer* $_r$, $1 \leqslant _r \leqslant n$,

$$P[\overline{X} \geqslant a, X_{(r)} \geqslant b] \geqslant P[\overline{X} \geqslant a] \, P[X_{(r)} \geqslant b] \qquad (4.1)$$

$$P[\overline{X} < a, X_{(r)} < b] \geqslant P[\overline{X} < a] \, P[X_{(r)} < b]. \qquad (4.2)$$

The lemma is an easy consequence of a general theorem (Esary, Proschan, and Walkup [10]). For easy reference, we quote the theorem below, as well as the definition of "associatedness." Random

TABLE VI. *Lower Limits used in Computation of Acceptance Probabilities for Exponential Distribution*

	n	k	Lower Limit L		
			$\alpha=0.10$	$\alpha=0.05$	$\alpha=0.01$
$\lambda=0.5$	5	0	0.0105	0.0051	0.0010
	5	1	.0594	.0398	.0168
	5	2	.1418	.1047	.0560
	5	3	.2689	.2097	.1255
	10	0	.0053	.0026	.0005
	10	1	.0280	.0186	.0078
	10	2	.0614	.0455	.0243
	10	3	.1038	.0813	.0488
	20	0	.0026	.0013	.0003
	20	1	.0136	.0091	.0038
	20	2	.0290	.0216	.0115
	20	3	.0473	.0370	.0222
	30	0	.0018	.0009	.0002
	30	1	.0090	.0060	.0025
	30	2	.0190	.0141	.0075
	30	3	.0306	.0240	.0145
$\lambda=1.0$	5	0	.0210	.0103	.0020
	5	1	.1188	.0796	.0336
	5	2	.2837	.2095	.1120
	5	3	.5379	.4193	.2510
	10	0	.0106	.0051	.0010
	10	1	.0560	.0372	.0156
	10	2	.1227	.0910	.0487
	10	3	.2076	.1625	.0976
	20	0	.0053	.0026	.0005
	20	1	.0273	.0182	.0076
	20	2	.0581	.0431	.0230
	20	3	.0945	.0740	.0445
	30	0	.0035	.0017	.0003
	30	1	.0180	.0121	.0050
	30	2	.0380	.0282	.0150
	30	3	.0612	.0479	.0289
$\lambda=2$	5	0	.0420	.0205	.0040
	5	1	.2376	.1592	.0671
	5	2	.5674	.4190	.2241
	5	3	1.0757	.8386	.5021
	10	0	.0211	.0102	.0020
	10	1	.1121	.0744	.0312
	10	2	.2455	.1820	.0973
	10	3	.4153	.3250	.1952
	20	0	.0105	.0051	.0010
	20	1	.0545	.0363	.0152
	20	2	.1161	.0862	.0459
	20	3	.1891	.1479	.0889
	30	0	.0070	.0034	.0007
	30	1	.0359	.0241	.0100
	30	2	.0760	.0564	.0300
	30	3	.1225	.0959	.0578

TABLE VII.   *Comparison of Approximation P_a with Simulation for $P[\overline{X} \geqslant \mu_0, N_L \leqslant k]$ where $P[N_L \leqslant k] = 1-\alpha$ for Exponential Distribution $E(\lambda, 0)$*

		Probability of Acceptance					
		$\alpha=0.10$		$\alpha=0.05$		$\alpha=0.01$	
n	k	P_a	Simul	P_a	Simul	P_a	Simul
$\lambda=0.5, \mu_0=0.25$							
5	0	0.781	0.825	0.850	0.853	0.868	0.893
5	1	.804	.846	.847	.871	.868	.896
5	2	.811	.857	.846	.874	.867	.897
5	3	.819	.869	.847	.885	.866	.899
10	0	.842	.875	.922	.929	.943	.957
10	1	.862	.889	.919	.927	.943	.958
10	2	.865	.893	.915	.933	.942	.958
10	3	.867	.897	.913	.935	.941	.956
20	0	.878	.902	.964	.948	.987	.985
20	1	.898	.905	.960	.954	.987	.984
20	2	.898	.907	.956	.955	.986	.984
20	3	.898	.899	.953	.948	.985	.984
30	0	.886	.901	.973	.952	.997	.987
30	1	.906	.904	.969	.951	.997	.990
30	2	.906	.903	.965	.948	.996	.990
30	3	.906	.903	.962	.950	.995	.989
$\lambda=1.0, \mu_0=0.75$							
5	0	.645	.632	.698	.651	.712	.686
5	1	.668	.657	.698	.660	.712	.689
5	2	.673	.665	.699	.667	.711	.690
5	3	.688	.676	.702	.674	.711	.691
10	0	.705	.712	.768	.754	.785	.776
10	1	.726	.726	.768	.761	.785	.777
10	2	.733	.734	.767	.766	.785	.777
10	3	.738	.745	.767	.769	.784	.778
20	0	.775	.789	.848	.846	.868	.873
20	1	.795	.800	.846	.849	.868	.876
20	2	.798	.804	.844	.849	.867	.875
20	3	.801	.806	.843	.851	.867	.873
30	0	.815	.839	.893	.890	.915	.920
30	1	.835	.846	.890	.887	.914	.921
30	2	.837	.842	.887	.884	.914	.922
30	3	.838	.846	.886	.891	.913	.921
$\lambda=2.0, \mu_0=0.75$							
5	0	.825	.872	.899	.915	.919	.950
5	1	.846	.883	.895	.927	.919	.954
5	2	.851	.891	.893	.929	.918	.953
5	3	.856	.894	.892	.935	.916	.955
10	0	.870	.894	.954	.944	.976	.987
10	1	.889	.889	.950	.944	.976	.987
10	2	.891	.898	.945	.948	.975	.986
10	3	.891	.894	.942	.945	.974	.985
20	0	.887	.902	.974	.952	.997	.991
20	1	.906	.903	.970	.956	.997	.989
20	2	.906	.905	.965	.956	.996	.991
20	3	.906	.904	.962	.955	.995	.992
30	0	.889	.907	.976	.956	1.000	.990
30	1	.909	.906	.972	.949	.999	.991
30	2	.908	.902	.968	.948	.999	.991
30	3	.908	.901	.965	.952	.998	.990

variables $X_1,...,X_n$ are said to be associated if

$$\text{Cov}(f(T), g(T)) \geqslant 0$$

for all non-decreasing functions f and g in each X_i for which $Ef(T)$, $Eg(T)$, $Ef(T)g(T)$ exist and T denotes $\{X_1,...,X_n\}$.

THEOREM 4.1. *Let* $T = \{X_1,...,X_n\}$ *be associated,* $S_i = f_i(T)$ *and* f_i *be nondecreasing for* i=1,...,k. *Then*

$$P[S_1 \leqslant s_1,...,S_k \leqslant s_k] \geqslant \prod_{i=1}^{k} P[S_i \leqslant s_i] \tag{4.3}$$

$$P[S_1 > s_1,...,S_k > s_k] \geqslant \prod_{i=1}^{k} P[S_i > s_i] \tag{4.4}$$

for all $s_1,...,s_k$.

PROOF OF LEMMA 4.1: In our case the X_i's are statistically independent and hence associated. Let $S_1 = \overline{X}$ and $S_2 = X_{(r)}$. Clearly, S_1 and S_2 are non-decreasing functions in each of the X_i's; hence (4.1) and (4.2) hold. Moreover, $\text{Cov}(S_1, S_2) = \text{Cov}(\overline{X}, X_{(r)}) \geqslant 0$. This completes the proof.

From Lemma 4.1, we have a lower bound $\underline{P}$ to the acceptance probability

$$\underline{P} = P[\overline{X} \geqslant a] P[X_{(k+1)} > L] \leqslant P_n = P[\overline{X} \geqslant a, X_{(k+1)} > L], \tag{4.5}$$

where $k + 1$ corresponds to r.

The r.v. $X_{(k+1)}$ can be transformed to a r.v. Z with Beta distribution with parameters $n-k$ and $k+1$. Thus

$$P[X_{(k+1)} > L] = P[Z < 1 - F_X(L)] = \frac{\Gamma(n+1)}{\Gamma(k+1)\Gamma(n-k)} \int_0^{1-p} z^{n-k-1}(1-z)^k dz. \tag{4.6}$$

The lower bound $\underline{P}$ in (4.5) can be computed using the marginal distribution of the sample mean and the Beta distribution.

Because the computation of the lower bound $\underline{P}$ is much easier than the computation of the acceptance probability P_n it would be an immense simplification if the lower bound could serve as an approximation for P_n.

Therefore, it is of practical importance to determine the sample size n and values of k that are necessary in order that the lower bound be an acceptable approximation for P_n. In other words, it is of interest to know the smallest value of n and the range of k values which makes the independence of $\overline{X}$ and $X_{(k+1)}$ acceptable.

5. Comparison of the Exact Probability of Acceptance with the Approximation and the Lower Bound

5.1 Acceptance Probability Curves

The acceptance probabilities computed using either simulation or numerical integration along with the corresponding lower bound $\underline{P}$ and the approximation P_a are plotted as a function of one parameter

of the distribution in question. This provides a comparison of the relative accuracy of P_a to $\underline{P}$ as a technique for approximating P_n. The curves are varied over n and k in order to examine the effect of sample size and number of allowable defectives k on P_n, P_a and $\underline{P}$.

5.2 Normal Distribution

Assuming that $X_1,\ldots, X_n$ are i.i.d. $N(\mu,1)$, the acceptance probability

$$P_n = P_\mu[\overline{X} \geqslant \mu_0, X_{(k+1)} > L]$$

for L chosen according to (3.2.3) and $\mu_0 = 0$ was computed using a technique for simulating random normal deviates due to Box and Muller [3]. The resulting acceptance probabilities as a function of μ are shown as the solid line in figures 1-4.

The corresponding lower bound $\underline{P}$ was computed from (4.5) and the approximation $\overline{P}_a$ was computed for (3.1.9).

The relationships among the probability of acceptance P_n, its approximation P_a, and its lower bound $\underline{P}$ as a function of sample size n and allowable number of defectives k is depicted in figures 1-4 for samples of size $n = 10$ and $n = 30$. The following convention is used for all figures; namely, P_n is shown as a solid line; P_a is shown as a heavy dashed line; and $\underline{P}$ is shown as a lighter dotted line.

From figure 1 it is obvious that when $k = 0$ and n is small, P_a is a better approximation to the acceptance probability than the lower bound as long as $\mu < 0.25$. As n increases the superiority of P_a to $\underline{P}$ increases as k is allowed to become larger. For example, when $k = 3$ as in figure 4, the lower bound
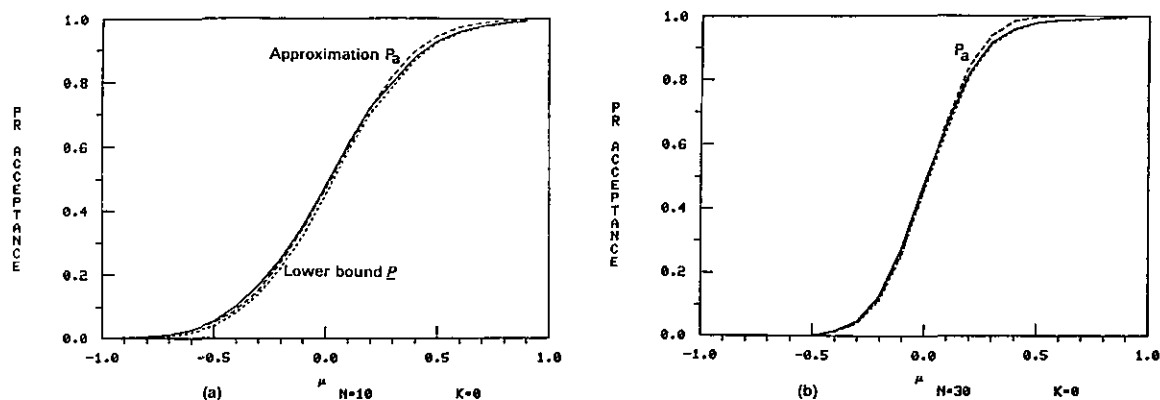
FIGURE 1.   Acceptance probabilities when the number of allowable defectives $k = 0$ and n observations are drawn from the normal distribution $N(\mu, 1)$.
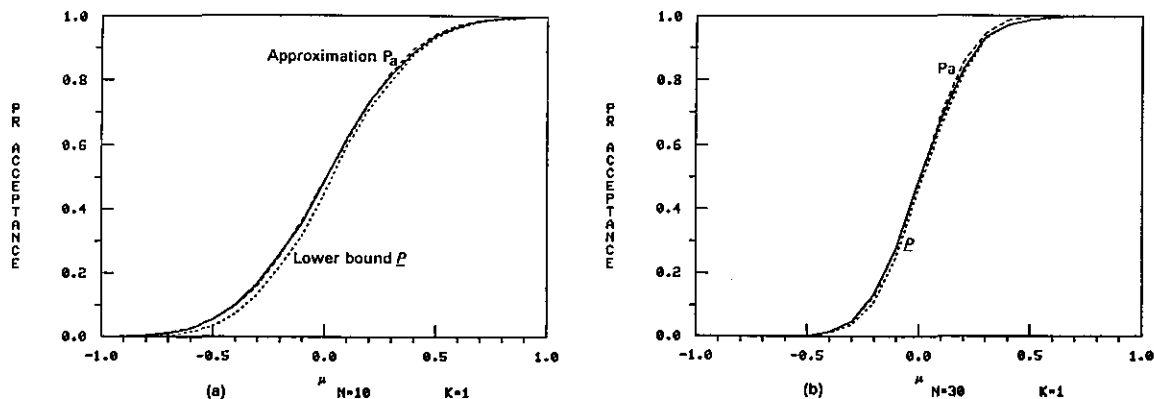
FIGURE 2.   Acceptance probabilities when the number of allowable defectives $k = 1$ and n observations are drawn from the normal distribution $N(\mu, 1)$.
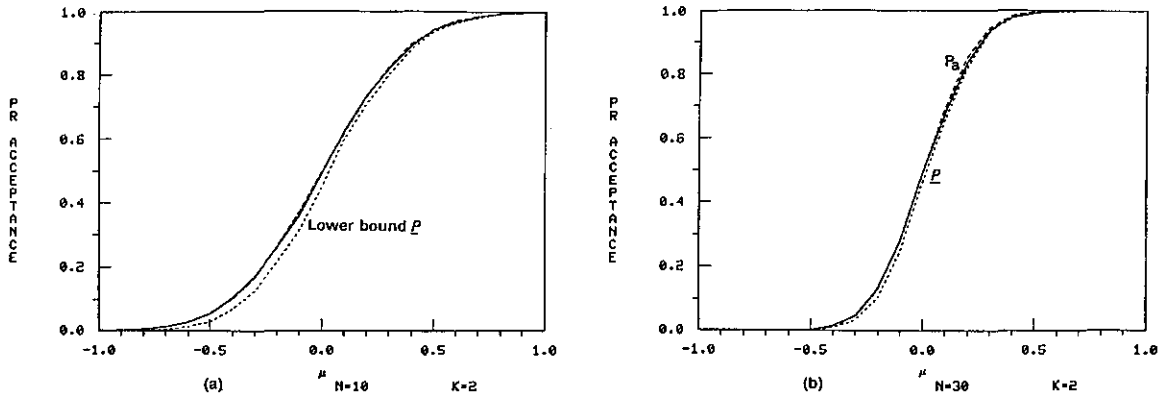
FIGURE 3. Acceptance probabilities when the number of allowable defectives $k = 2$ and n observations are drawn from the normal distribution $N(\mu, 1)$.
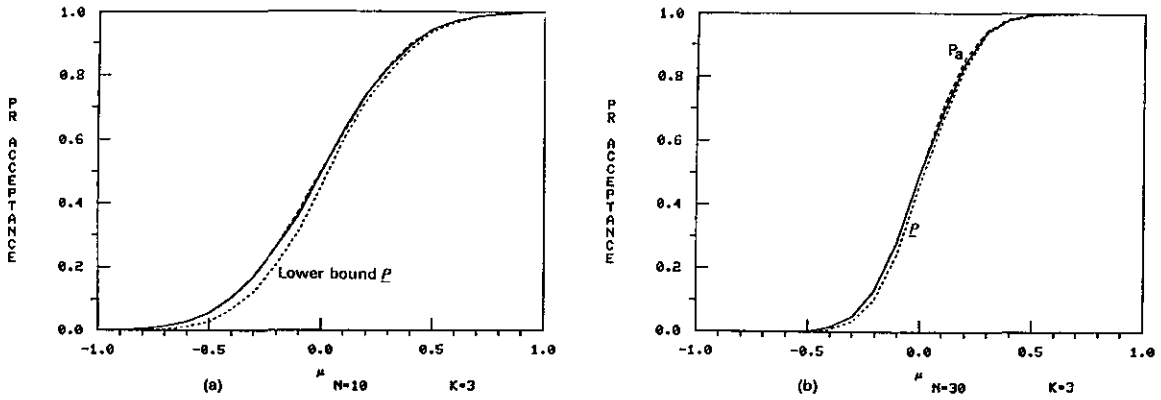
FIGURE 4. Acceptance probabilities when the number of allowable defectives $k = 3$ and n observations are drawn from the normal distribution $N(\mu, 1)$.

does not give a satisfactory approximation for the smaller sample size, and P_a is clearly preferable. Even for $n = 30$, P_a is at least as accurate as $\underline{P}$ over the entire range of μ.

5.3 Weibull Distribution

Assuming that $X_1,...,X_n$ are i.i.d. $W(1,\theta)$, and that $\mu_0 = 0.75$ and that L is chosen according to (3.3.8) with $\theta = 1$, the acceptance probability was computed by simulation and is shown as the solid line in figures 5-8. The corresponding lower bound $\underline{P}$ was also computed using simulation and is
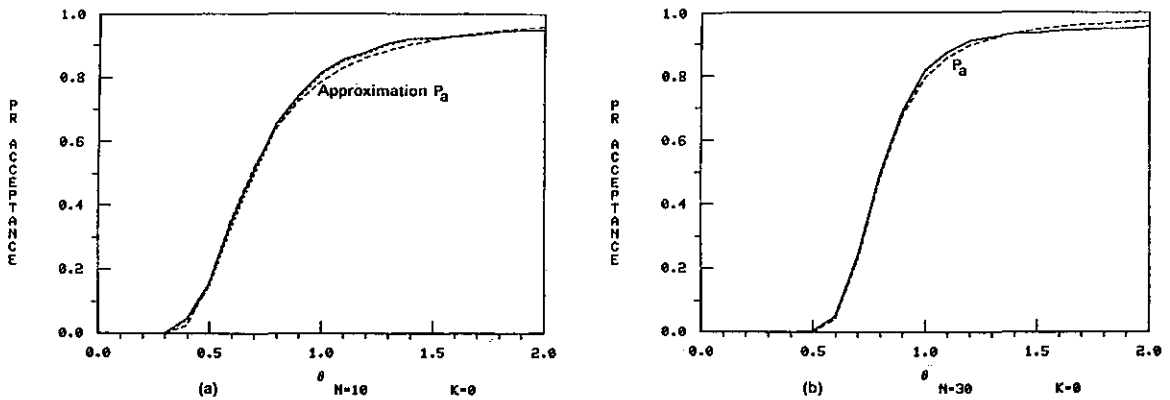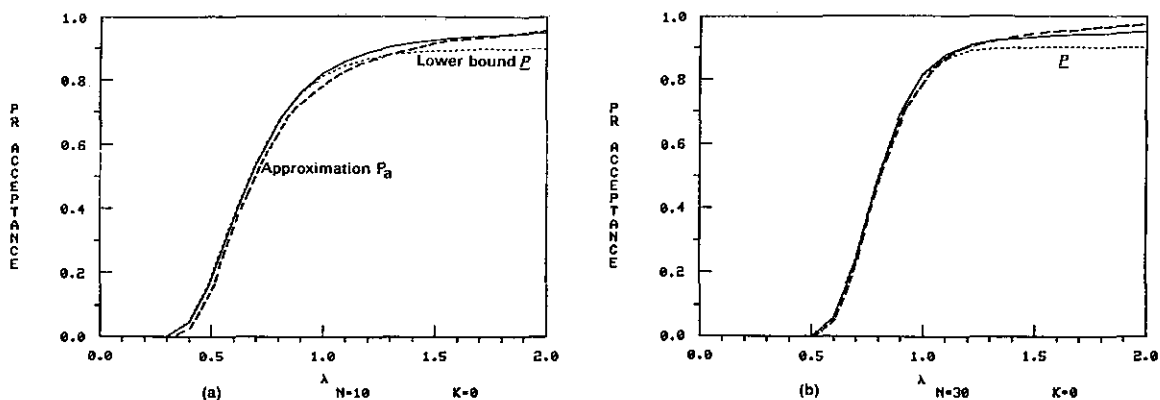

FIGURE 5. Acceptance probabilities when the number of allowable defectives $k = 0$ and n observations are drawn from a Weibull distribution $W(1, \theta)$.

501
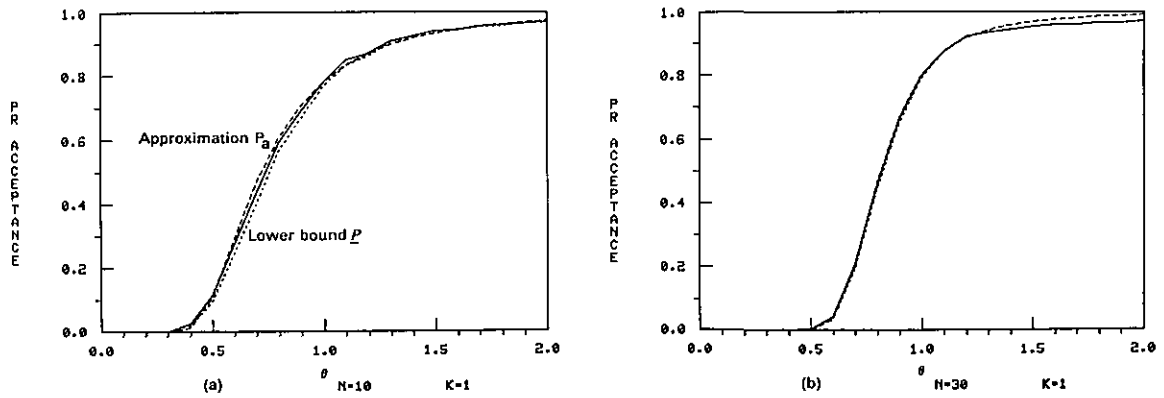
FIGURE 6.   Acceptance probabilities when the number of allowable defectives $k = 1$ and n observations are drawn from a Weibull distribution $W(1, \theta)$.
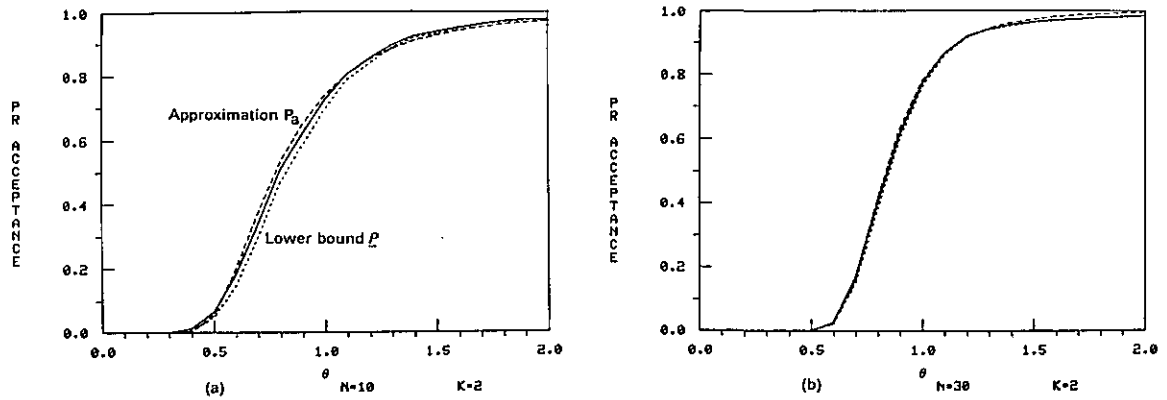
FIGURE 7.   Acceptance probabilities when the number of allowable defectives $k = 2$ and n observations are drawn from a Weibull distribution $W(1, \theta)$.
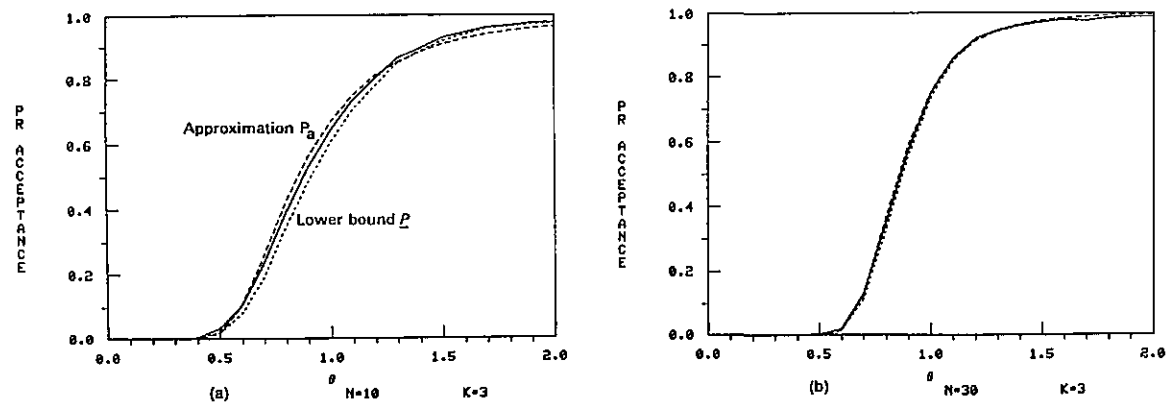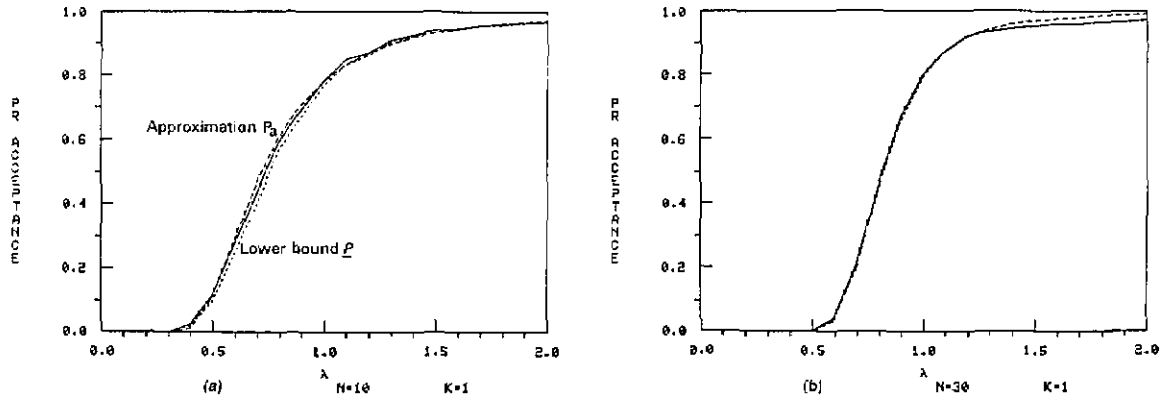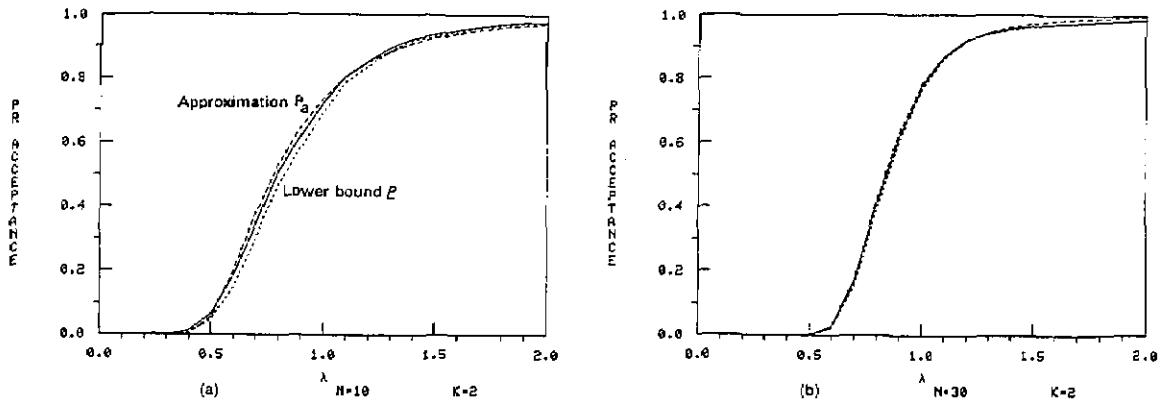

FIGURE 8.   Acceptance probabilities when the number of allowable defectives $k = 3$ and n observations are drawn from a Weibull distribution $W(1, \theta)$.

represented by the dotted line in the same figures. The approximation P_a is shown by the heavy dashed line in the figures.

The figures show that P_a is not a particularly good approximation to P_n when $k = 0$, and one would do much better using the lower bound $\underline{P}$. However, P_a shows the same characteristic for the Weibull distribution as for the normal distribution; namely, that as k/n increases the accuracy of the approximation increases. For $n = 10$ and $k = 3$, P_a is superior to $\underline{P}$; for $n = 30$, $\underline{P}$ is indistinguishable from the simulated acceptance probability.

5.4 Exponential Distribution

5.4.1 Comparison with a UMP Test

As discussed in section 1, we may view the problem of finding an optimal sampling procedure as a hypothesis testing problem formulated in (1.4). In general there exists no uniformly most powerful (UMP) test for (1.4). However, it is interesting to note that in the exponential distribution the dual acceptance criterion for $k = 0$ corresponds to a test which is UMP for a subset of alternatives specified in (1.4). Specifically, suppose the sample comes from the exponential pdf given in (3.4.1).

The UMP acceptance region for testing

$$H_0: \lambda = \lambda^* \text{ and } \beta = \beta^*$$

versus

$$H_1: 0 < \lambda < \lambda^* \text{ and } 0 < \beta < \beta^*$$

is given by

$$[\overline{X} \geqslant \mu_0, X_{(1)} \geqslant \beta^*]. \tag{5.4.1}$$

This testing problem is equivalent to testing

$$H_0: \lambda = \lambda^* \text{ and } p = p^*$$

versus

$$H_1: 0 < \lambda < \lambda^* \text{ and } p > 1 - (1-p^*)^{\lambda^*/\lambda}$$

where

$$p^* = 1 - \exp\{-(L-\beta^*)/\lambda^*\}$$

or

$$\beta^* = L + \lambda^* \log (1-p^*).$$

Under H_0, $P_{\lambda^*,\beta^*}[X_{(1)} \geqslant \beta^*] = 1$, and μ_0 is determined by the equation

$$P_{\lambda^*,\beta^*}[\overline{X} \geqslant \mu_0] = 1-\alpha, \tag{5.4.2}$$

where α is a predetermined level of significance (Lehmann [15]).

If we set $L = \beta^*$ and $k = 0$, the test specified by (5.4.1) clearly is the same test specified by (1.3), and the acceptance probability

$$P_n = P_{\lambda,\beta} \{\overline{X} \geqslant \mu_0, X_{(1)} \geqslant \beta^*\} \tag{5.4.3}$$

can be computed either by the approximation shown in section 3.4 or by numerical integration using an exact formula for the distribution of $\overline{X}$ and N_L as shown in the next section.

5.4.2 Exact Distribution of $\overline{X}$ and N_L

The joint distribution of $\overline{X}$ and N_L can be obtained from the order statistics.

Let

$$Z_1 = nX_{(1)}$$

$$Z_i = (n-i+1)(X_{(i)} - X_{(i-1)}).$$

We have the pdf of $Z_{(1)}$,

$$g_1(z_1) = \lambda^{-1} \exp\{-(z_1 - n\beta)/\lambda\}, z_1 > \beta \qquad (5.4.4)$$

and for $i \geq 2$, Z_i has a pdf

$$g_i(z_i) = \lambda^{-1} \exp(-z_i/\lambda), z_i \geq 0.$$

To compute the acceptance probability P_n for an arbitrary k, we make use of the fact that the Z's are independent r.v.'s, and that

$\sum\limits_{j=1}^{n} X_j = \sum\limits_{j=1}^{n} Z_j = \sum\limits_{j=1}^{n} X_{(j)}$ and proceed as follows:

$$P_n = P_{\lambda,\beta} [\overline{X} \geq \mu_0, N_L \leq k]$$

$$= \int \cdots \int_A P[\sum_1^n Z_i \geq n\mu_0, \sum_1^{k+1} Z_i/(n-i+1) > L \bigg| z_1, \cdots, z_{k+1}] \left\{ \prod_1^{k+1} g_i(z_i) \right\} dz_1 \cdots dz_{k+1}$$

$$= \int \cdots \int_A P[\sum_{k+2}^n Z_i \geq n\mu_0 - \sum_1^{k+1} z_i] \left\{ \prod_1^{k+1} g_i(z_i) \right\} dz_1 \cdots dz_{k+1} \qquad (5.4.5)$$

where $A = \{(z_1, \cdots, z_{k+1}): \sum_1^{k+1} z_i/(n-i+1) > L$ and $n\mu_0 - \sum_1^{k+1} z_i \geq 0\}$.

The expression in (5.4.5) is the exact probability of acceptance, P_n.

When $k = 0$, the computation of P_n reduces to

$$P_n = \int_{nL}^{n\mu_0} P[\sum_2^n Z_i \geq n\mu_0 - z_1] g_1(z_1) dz_1 + \int_{n\mu_0}^{\infty} g_1(z_1) dz_1. \qquad (5.4.6)$$

Note that the sum $Y = \sum\limits_2^n Z_i$ has a gamma density.

$$f(y) = \frac{(1/\lambda)^{n-1}}{\Gamma(n-1)} y^{n-2} \exp(-y/\lambda). \qquad (5.4.7)$$

Substituting (5.4.4) and (5.4.7) in (5.4.6) we obtain

$$P_n = \frac{1}{\Gamma(n-1)} \int_a^b \int_c^{\infty} e^{-v} v^{n-2} \exp\{-(z_1 - n\beta)/\lambda\} dv dz_1 + \exp\{-n(\mu_0 - \beta)/\lambda\} \qquad (5.4.8)$$

where

$$a = nL$$
$$b = n\mu_0$$
$$c = (n\mu_0 - z_1)/\lambda$$

The lower bound for P_n is

$$\underline{P} = \int_{2n(\mu_0 - \beta)/\lambda}^{\infty} f(x) dx \int_{2n(L-\beta)/\lambda}^{\infty} g(x) dx \qquad (5.4.9)$$

where $f(x)$ is the pdf of the $\chi^2(2n)$ and $g(x)$ is the pdf of the $\chi^2(2)$.

5.4.3 Acceptance probabilities

If we assume that $X_1, \cdots, X_n$ are i.i.d. $E(\lambda, 0)$, the acceptance probability for $k = 0$

$$P_n = P_\lambda[\overline{X} \geqslant \mu_0, N_L \leqslant 0] = P[\overline{X} \geqslant \mu_0, X_{(1)} > L]$$

is computed from (5.4.8) using a numerical integration technique that takes advantage of the fact that the inner integral is an incomplete Γ-function. Note that μ_0 is determined from $\chi^2(2)$ according to (5.4.2), and L is determined according to (3.4.5). The acceptance probability P_n is shown as the solid line in figure 9.

FIGURE 9. Acceptance probabilities when the number of allowable defectives $k = 0$ and n observations are drawn from an exponential distribution $E(\lambda, 0)$.

The acceptance probabilities for $k = 1,2,3$, for $\mu_0 = 0.75$ and L chosen according to (3.4.5) were computed by simulation as were the corresponding values of $\underline{P}$. The approximation P_a was computed from (3.4.6). Results are shown in figures 10-12.

The graphs show that P_a is a better approximation to P_n than the lower bound $\underline{P}$ for small sample size where the superiority of P_a over $\underline{P}$ increases as k increases. For large sample size, say $n = 30$, the two methods give almost identical approximations to P_n.

Values of μ_0 used in Computation of
Acceptance Probabilities for UMP Test for
Exponential Distribution

	Values of μ_0		
n	$\alpha=0.10$	$\alpha=0.05$	$\alpha=0.01$
5	0.48652	0.39403	0.25582
10	0.62213	0.64254	0.41302
20	0.77626	0.66273	0.55411
30	0.77431	0.71998	0.62475

FIGURE 10. Acceptance probabilities when the number of allowable defectives $k = 1$ and n observations are drawn from an exponential distribution $E(\lambda, 0)$.

FIGURE 11. Acceptance probabilities when the number of allowable defectives $k = 2$ and n observations are drawn from an exponential distribution $E(\lambda, 0)$.
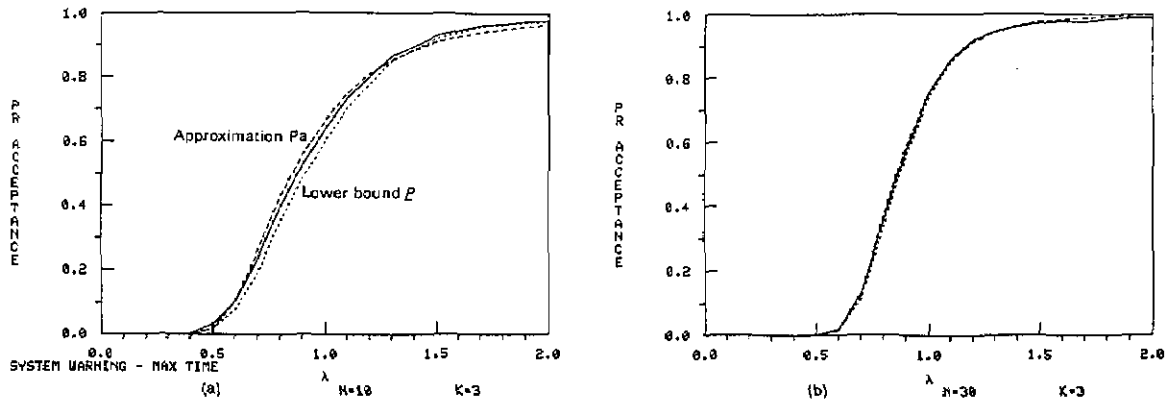
FIGURE 12. Acceptance probabilities when the number of allowable defectives $k = 3$ and n observations are drawn from an exponential distribution $E(\lambda, 0)$.

6. Synopsis

The problem of computing the acceptance probability P_n has been addressed by an approximation P_a that relies on the asymptotic joint distribution of the sample mean and number of defectives in the sample. P_a has the advantage that it is applicable to any continuous distribution. It is computed using

506

a $N(0,1)$ cdf and a bivariate normal cdf which in turn can be reduced to a single variable integration.

The approximation P_a compares very favorably with another published approximation for the normal distribution and with a lower bound $\underline{P}$. Graphs of the acceptance probability as a function of one parameter of the distribution are used to compare the relative accuracies of P_a and $\underline{P}$. The graphs show that for the normal distribution P_a and $\underline{P}$ have comparable accuracies with k = 0. As k/n increases, P_a quickly becomes superior to $\underline{P}$, and even for large n and $k > 0$ P_a is superior. In other words, the best results for the normal distribution are obtained with $\underline{P}$ when k = 0 and with P_a for all other values of k.

In the case of Weibull distribution $\underline{P}$ is superior for $k = 0$. As k/n increases, P_a gains in accuracy, and for large n, P continues to have an edge over P_a. The difficulty in computing P for the Weibull distribution may make it desirable to use P_a for all applications.

In the case of exponential distribution, the exact joint distribution of the sample mean and number of defectives in the sample has been derived for $k = 0$. The computation of the acceptance probability P_n in this case involves a two-variable integration. Graphs of the acceptance probabilities show that the lower limit $\underline{P}$ gives a consistently good approximation to the acceptance probability. The approximation P_a and the lower limit $\underline{P}$ have also been computed for the exponential distribution for $1 \leqslant k \leqslant 3$. The graphs for these tests show that $\underline{P}$ is comparable or superior to P_a for large $n(n \geqslant 30)$ with P_a being somewhat superior when n is small, say $n \leqslant 10$.

7. References

[1] American Society for Testing and Materials. C825-79 Standard Specifications for Precast Concrete Barrier.

[2] Anderson, T.W. (1958). *An Introduction to Multivariate Statistical Analysis*. John Wiley & Sons, Inc: New York.

[3] Box, G.P. and Muller, M.E. (1958). A note on the generation of random normal deviates. JACM. pp. 620-611.

[4] Brickenkamp, C.S., Hasko, S., Natrella, M.G. (1981). Checking the Net Contents of Packaged Goods. NBS Handbook 133. U.S. Government Printing Office: Washington. pp. 2-7.

[5] Broussalian et al. (1975). Considerations in the Use of Sampling Plans for Effecting Compliance with Mandatory Safety Standards. NBSIR 75-697. National Bureau of Standards, Gaithersburg, MD.

[6] Chung, K.L. (1960). *Markov Chains with Stationary Transition Probabilities*. Springer-Verlag: Berlin. p. 84.

[7] Eisenberger, I. (1968). Testing the Mean and Standard Deviation of a Normal Distribution Using Quantiles. Technometrics. 10 (4) pp. 781-91.

[8] Elder, Robert S. and Muse, H. David (1982). An Approximate Method for Evaluating Mixed Sampling Plans. Technometrics, 24(3), pp. 207-212.

[9] Environmental Protection Agency (1971). National primary and secondary ambient air quality standards. Federal Register, 36(84). pp. 8186-8201.

[10] Esary, J.D., Proschan, F. and Walkup, D.W. (1967). Association of Random Variables with Applications. Annals of Math Stat, 38. pp. 1466-1474.

[11] Gross, A.J. and Clark, V.A. (1975). *Survival Distributions: Reliability Applications in the Biomedical Sciences*. John Wiley & Sons, Inc: New York pp. 14-18.

[12] Harter, H. Leon. (1964). *New Tables of the Incomplete Gamma-Function Ratio and of Percentage Points of the Chi-square and Beta Distributions*. US Government Printing Office: Washington.

[13] Johnson, N.L. and Kotz, S. (1970). *Continuous Univariate Distributions — 1*. Houghton Mifflin Co: Boston. pp. 251-252.

[14] Lauer, G.N. (1982). Probabilities of Noncompliance for Sampling Plans in NBS Handbook 133. Journal of Quality Tech, 14 (3). pp. 162-165.

[15] Lehmann, E.L. (1959). *Testing Statistical Hypotheses*. John Wiley & Sons, Inc.: New York. p. 110.

[16] Pearson, E.S. and Hartley, H.O. (1969). *Biometrika Tables for Statisticians*, Vol. I (1st edition). University Press: Cambridge. p. 43.

[17] Perlman, M.D. (1980). Unbiasedness of likelihood ratio tests for equality of several covariance matrices and equality of several multivariate normal populations. Annals of Stat, 8(2). pp. 247-263.

[18] Perng, S.A. (1977). An Asymptotically Efficient Test for the Location Parameter and the Scale Parameter of an Exponential Distribution. Comm in Stat. Theory and Methods, A6 (14). pp. 1399-1407.

[19] Schilling, E.G. and Dodge, H.F. (1969). Procedures and Tables for Evaluating Dependent Mixed Acceptance Sampling Plans. Technometrics, 11(2). pp. 341-372.

[20] Tables of the Bivariate Normal Distribution Function and Related Functions. (1959). NBS AMS 50. US Government Printing Office: Washington. pp. vi-vii.

[21] Weed, R.M. (1982). Bounds for Correlated Compound Probabilities. Journal of Quality Tech. 14(4). pp. 196-200.

[22] Weed, R.M. (1980). Analysis of Multiple Acceptance Criteria. Trans. Research Record, 745 pp. 20-23.

8. Appendix A

The approximation P_a given in (3.1.9) involves the computation of $L(a,b,\varrho)$ defined as

$$L(a,b,\varrho) = \int_a^\infty \int_b^\infty g(z,y,\varrho)dydz.$$

The computation of $L(a,b,\varrho)$ can be reduced to a single variable integration. When a and b are both positive [18],

$$L(a,b,\varrho) = \frac{1}{2\pi} \int_{\arccos\varrho}^\pi \exp\{-\tfrac{1}{2}(a^2+b^2-2ab\cos w)\,\mathrm{cosec}^2w\}dw$$

The following recursion relations hold:

$$L(-a,b,\varrho) \quad = \quad -L(a,b,-\varrho) + \tfrac{1}{2}[1-h(b)]$$

$$L(a,-b,\varrho) \quad = \quad -L(a,b,-\varrho) + \tfrac{1}{2}[1-h(a)]$$

$$L(-a,-b,\varrho) \quad = \quad L(a,b,\varrho) + \tfrac{1}{2}[h(a)+h(b)]$$

$$\text{where } h(x) \quad = \quad \int_{-x}^x \exp(-t^2/2)dt.$$

The approximation P_a can be computed for all values of a,b and ϱ using the foregoing equations.

$$P_a \;=\; \Phi(-a) - L(a,b,\varrho), a>0, b>0$$

$$P_a \;=\; \Phi(-a) - \Phi(-b) + L(-a,b,-\varrho), a<0, b>0$$

$$P_a \;=\; L(a,-b,-\varrho), a>0, b<0$$

$$P_a \;=\; \Phi(b) - L(-a,-b,\varrho), a<0, b<0$$

where $\Phi(x) = \int_{-\infty}^x \exp(-t^2/2)dt$.

9. Appendix B

Asymptotic independence of the sample mean and the $(n-k)^{\text{th}}$ extreme statistic.

Let $X_1,\cdots, X_n$ be i.i.d with a p.d.f. $f(x)$. Denote the c.d.f. of the X's by $F(x)$. Assume that X's have a finite mean μ and finite variance σ^2. Let $X_{(1)} < \cdots < X_{(n)}$ be the order statistics.

The conditional density of $X_{(1)},\cdots, X_{(n)}$ given that $X_{(n-k)} = x_{(n-k)}$ is given by

$$L_{x_{(n-k)}} = \frac{(n-k-1)! \prod\limits^{n-k-1}_{1} f(x_{(i)})}{\{F(x_{(n-k)})\}^{n-k-1}} \cdot \frac{k! \prod\limits^{n}_{n-k+1} f(x_{(i)})}{\{1-F(x_{(n-k)})\}^{k}} \tag{1}$$

Clearly, given that $X_{(n-k)} = x_{(n-k)}$, the joint conditional density may be regarded as the joint density of two dependent samples $\{Y_1, \cdots, Y_{n-k-1}\}$ and $\{W_1, \cdots, W_k\}$, where the Y-sample has a p.d.f.

$$\begin{aligned} h(x) &= \frac{f(x)}{F(x_{(n-k)})} \quad , \text{ if } x < x_{(n-k)} \\ &= 0 \quad\quad , \text{ if } x > x_{(n-k)} \end{aligned} \tag{2}$$

and the W-sample has a p.d.f.

$$\begin{aligned} g(x) &= \frac{f(x)}{1-F(x_{(n-k)})} \quad , \text{ if } x > x_{(n-k)} \\ &= 0 \quad\quad , \text{ if } x < x_{(n-k)} \end{aligned} \tag{3}$$

THEOREM. *For every fixed k, $\sqrt{n}(\bar{X}-\mu)$ is asymptotically independent of* $X_{(n-k)}$ *as* $n \to \infty$.

PROOF: Rewrite $\bar{X}$ in terms of the Y's and the W's. We obtain

$$\frac{\sqrt{n}(\bar{X}-\mu)}{\sigma} = \frac{\sqrt{n-k-1}\,(\bar{Y}-\mu)}{\sigma}\frac{\sqrt{n-k-1}}{\sqrt{n}} + \frac{(\bar{W}-\mu)\,k}{\sigma\sqrt{n}} + \frac{X_{(n-k)}-\mu}{\sigma\sqrt{n}} \tag{4}$$

From (2) we have

$$EY_i-\mu = \frac{\int\limits_0^{x_{(n-k)}} x\,dF(x)\int\limits_{x_{(n-k)}}^{\infty} dF(x)}{F(x_{(n-k)})} - \int\limits_{x_{(n-k)}}^{\infty} x\,dF(x) \tag{5}$$

Making use of (4) and (5), and letting A be the value of EY_i with $X_{(n-k)}$ replaced by $X_{(n-k)}$, we get

$$\frac{\sqrt{n}(\bar{X}-\mu)}{\sigma} = \frac{\sqrt{n-k-1}}{\sigma}\frac{(\bar{Y}-EY_i)}{\sigma}\frac{\sqrt{n-k-1}}{\sqrt{n}}$$

$$+ \frac{(n-k-1)\,(A-\mu)}{\sqrt{n}\sigma} + \frac{(\bar{W}-\mu)}{\sigma}\frac{k}{\sqrt{n}} + \frac{X_{(n-k)}-\mu}{\sigma\sqrt{n}}$$

Since k is fixed, clearly $(\bar{W}-\mu)\ k/\sigma\sqrt{n} \to 0$ in probability as $n \to \infty$. To prove the theorem we need the following two lemmas in which we show that the second and the fourth terms tend to zero in probability. Then the theorem follows from the fact that the first term converges in distribution to $N(0,1)$ which is the "unconditional" limiting distribution of $\sqrt{n}(\bar{X}-\mu)$.

LEMMA 1. *As* n → ∞,

$$\frac{X_{(n-k)}}{\sqrt{n}} \to 0 \; in \; P.$$

PROOF: For every $\varepsilon > 0$ and for a fixed k, it follows from the Chebychev inequality that

$$P\left\{\frac{|X_{(n-k)}|}{\sqrt{n}} > \varepsilon\right\} \leqslant \frac{E(X_{(n-k)})^2}{n\varepsilon^2} \leqslant \frac{1}{n\varepsilon} \; E(\max_{1\leqslant j\leqslant n} X_j^2)$$

Let $Y_j = X_j^2$ and $H(y) = P[Y_j \geqslant y]$.

Following a proof in Chung (1960),

$$P[\max_{1\leqslant j\leqslant n} Y_j \geqslant y] = 1 - [H(y)]^n \geqslant n[1-H(y)]$$

and

$$\frac{1}{n} E\{\max_{1\leqslant j\leqslant n} X_j^2\} = \frac{1}{n} \int_0^\infty \{1-[H(y)]^n\} \, dy \geqslant \int_0^\infty [1-H(y)]dy < \infty$$

On the other hand,

$$\frac{1}{n} E\{\max_{1\leqslant j\leqslant n} X_j^2\} = \int_0^\infty \int_{H(y)}^1 u^{n-1} \, du \, dy.$$

Since the expectation is finite, we can take the limit as $n \to \infty$ under the integral sign. As a result

$$\lim_{n\to\infty} \frac{1}{n} E\{\max_{1\leqslant j\leqslant n} X_j^2\} = \int_0^\infty \int_{H(y)}^1 \lim_{n\to\infty} u^{n-1} \, du \, dy = 0$$

LEMMA 2. For a fixed k, $0 \leqslant k \leqslant n-1$,

$$\overline{\sqrt{n-k-1}} \int_{X_{(n-k)}}^\infty x \, dF(x) \to 0 \; in \; P \; as \; n \to \infty.$$

PROOF: Since

$$\sqrt{n-k-1} \int_{X_{(n-k)}}^\infty x \, dF(x) = \sqrt{n-k-1} \, X_{(n-k)} \, [1-F(X_{(n-k)})]$$

$$+ \sqrt{n-k-1} \int_{X_{(n-k)}}^\infty [1-F(x)] \, dx, \tag{8}$$

we will show that each term on the right side of (8) converges in probability to zero.

Set

$$z = 1 - \frac{x}{n-k-1} \tag{9}$$

Then

$$P\{(n-k-1)[1-F(X_{(n-k)})] > x\} = \sum_{i=n-k}^{n} \binom{n}{i} z^i (1-z)^{n-i} \rightarrow e^{-x} \sum_{i=0}^{k} \frac{x^i}{i!} \tag{10}$$

We see that $X_{(n-k)}/\sqrt{n-k-1} \rightarrow 0$ in P as shown in Lemma 1 and $(n-k-1) [1-F(X_{(n-k)})]$ converges in distribution as shown in (10). Thus, the first term on the right side of (8) tends to zero in $\underline{P}$.

Finally, to show that the last term in (8) tends to zero in P, write this term as

$$\sqrt{n-k-1} \int_{X_{(n-k)}}^{\infty} [1-F(X)] \, dx = \sqrt{n-k-1)(1-F(X_{(n-k)})} \left\{ \int_{X_{(n-k)}}^{\infty} ([1-F(x)]dx) / \sqrt{1-F(X_{(n-k)})} \right\}$$

Clearly, the part in brackets tends to zero in P can be seen by the application of the L'Hospitals's rule to it.

Mathematical Analysis for Radiometric Calorimetry of a Radiating Sphere

L. A. Schmid*

National Bureau of Standards, Washington, DC 20234

Equations are derived from which the temperature dependence of both the specific heat and the thermal diffusivity of a spherical sample of material can be calculated from observations of the time dependence of the surface temperature and the time-rate of energy loss from the sample as it cools. The derivation takes into account the nonuniformity of the interior temperature field of the sample, and the resulting equations can be applied not only to radiative cooling, but also to any other cooling mechanism that does not violate the assumed spherical symmetry. The analysis excludes change of phase, but it does take thermal expansion into account. To permit the making of estimates necessary for the design of radiative cooling experiments, a universal temperature-time cooling curve is derived for the post-transient cooling regime of a radiating sphere of any size with arbitrary, but constant, thermal parameters.

Key words: calorimetry; Fourier equation; radiative cooling; specific heat; thermal diffusivity.

1. Introduction

The analysis presented in this paper is an outgrowth of a proposal made by J. H. Colwell [1,2] to determine the high-temperature values of the specific heat, thermal diffusivity, and total hemispherical emissivity of a spherical sample of refractory material by making independent optical observations of the surface temperature of the sample and its time-rate of energy loss as it cools by free radiation into a cold vacuum. The original proposal was made in the context of an experiment to be conducted on board the space shuttle, and envisaged induction heating of the sample. With this mode of heating, the total heat content of the spherical sample and its interior temperature field at the start of the observational run would be unknown. However, after an interval on the order of the characteristic thermal decay time of the sample, the interior temperature field would settle into the "post-transient regime" in which the interior field would be entirely determined by the time-dependence of the surface-temperature. Thus, in the post-transient regime it should, in principle, be possible to determine the temperature dependence of the thermal parameters from

a knowledge of the time dependence of the surface temperature and the rate of energy loss. The determination of the emissivity is a trivial matter, since it is proportional to the rate of energy loss divided by the fourth power of the surface temperature.

Stated in mathematical terms, the cooling sample could be regarded as mapping the temperature-dependent specific heat and diffusivity over into the time-dependent surface temperature and energy loss functions, and the analytical problem then consists of inverting this mapping so as to be able to express the two unknown thermal parameters in terms of the two observed time functions. The first step in carrying out this inversion, the results of which are summarized in section 2, is to find the "surface-driven solution" of the Fourier equation for specified temperature-dependent specific heat and thermal diffusivity. This solution is completely specified by the time dependence of the surface temperature, and the time rate of change of the total heat content can be calculated from it. If this calculated rate of change is then equated to the fourth power of the surface temperature in accordance with the Stefan-Boltzmann radiation law, a nonlinear *ordinary* differential equation (of infinite order) results which can be iteratively solved (in truncated form) for the case of con-

---

*Center for Chemical Engineering, National Engineering Laboratory

stant thermal parameters to yield a universal temperature versus time dependence for the post-transient regime. This solution, which is presented in section 3, is useful for making the various estimates that are necessary for the design of a radiative-cooling calorimetry experiment. At the end of section 3 an integral equation is given that could also be used as the basis of an iterative solution of the post-transient predictive problem.

In section 4 the surface-driven solution that is summarized in section 2 is inverted so as to yield expressions for specific heat and diffusivity in terms of the observed time-dependent surface temperature and time-rate of energy loss. These expressions constitute the desired solution of the calorimetric problem. The thermal parameters are expressed both in terms of truncated expansions whose coefficients involve higher-order time derivatives of the observed functions, as well as in terms of integral expressions involving retrospective weighted averages of the observed time-dependent functions. The truncated expansions, which are easier to apply than the integral expressions, ought to suffice for analyzing most post-transient experiments. In fact, in many experiments the simple approximate expressions given in eqs (44) and (45) will be sufficiently accurate. In section 4 an estimate of the range of validity of these simple expressions, as well as the range of validity of the more accurate truncated expansions, is given in terms of the magnitude of a suitably scaled dimensionless temperature. The scaling factor, which is introduced in section 3, takes the material parameters and sphere size into account. When these parameters have values for which the truncated expansions are not accurate, then the integral expressions for the thermal parameters can be used as a basis for an iterative solution of the calorimetric problem. These integral expressions could also be used to analyze a calorimetry experiment conducted in the transient regime, assuming that the knowledge of the surface temperature of the sample includes an interval (on the order of the characteristic decay time) that precedes the commencement of the cooling observations. For example, if a sample were held in a constant-temperature oven (of known temperature) long enough to become isothermal, and then suddenly removed to commence cooling which was observed for a time interval on the order of the characteristic thermal decay time, the integral expressions for the thermal parameters could be used to analyze the data.

Although the analysis of this paper was carried out with radiative cooling in mind, only in the solution of the predictive problem in section 3 is the radiative cooling law invoked. In the analysis of the calorimetric problem, the cooling law is never specified. All that is assumed is that the time dependence of the time-rate of total energy loss by the sample is known (as is the time dependence of the surface temperature).

The most obvious limitation of the analysis of this paper (aside from its restriction to spherical symmetry) is the exclusion of the possibility of phase change. That is, the spherical sample is assumed to be either entirely solid or entirely liquid throughout the experiment. In addition to this limitation, the analysis incorporates two approximations, the more significant being the neglect of the spatial variation of the diffusivity in the interior of the spherical sample. That is, the diffusivity is assumed to be a function of the *surface* temperature (which is a function only of time) rather than a function of the *interior* temperature (which is a function of the radial coordinate as well as of time). It is shown in section 2 that this approximation amounts to neglecting a very small term in the Fourier equation that has the form of an effective heat source, but, as explained in section 5, this effective heat source can be taken into account (if necessary) by a simple iterative procedure. The other approximation, whose effect is *completely negligible*, is the *neglect of the spatial variation of the mass density of the sample*. That is, the overall change in average density with temperature is taken into account, but at each instant the density throughout the sample is assumed to be spatially constant. In other words, as in the case of diffusivity, the density throughout the sample is assumed to be a function of the surface temperature rather than of the interior temperature.

The literature relevant to predictive solutions of the Fourier equation is old, vast, and still growing [3,4]. However, this literature is almost exclusively devoted to the initial-value approach to the problem which requires that at some instant the interior temperature field must have some exactly specified form (most commonly, a given uniform temperature). This point of view, however, is physically inappropriate to the calorimetric problem because what is usually known is the history of the environment to which the sample has been exposed (i.e., the history of its surface temperature), and not the interior temperature field at any instant. It is true that, if the sample is kept in a constant-temperature oven long enough, its interior temperature will indeed be spatially uniform, but this is a special case. It would be physically more natural to replace the initial specification of the interior temperature field with the specification of the surface temperature history back to $t = -\infty$. (It is shown in section 2 that as a practical matter it is only necessary to know the surface temperature during a very short period of the past.) There is a well-known solution to the Fourier equation (cf. for example p. 247 of Ref. [3]), which has the form of a convolution of the surface

temperature with the well-known diffusion kernel, but this solution is inappropriate to the calorimetry problem because it has a singularity at the center, and so (in the absence of a point heat source) can only be used to describe the temperature field in an infinite medium surrounding a spherical cavity.

The mathematical literature that is directly relevant to the determination of the thermal parameters from the observed surface temperature [5-13] unfortunately has remained within the framework of the initial-value approach. Because an arbitrarily specified time-dependence for the surface temperature is generally inconsistent with a previously specified initial interior temperature field, the problem is over-specified, and certain compatibility conditions must be satisfied before the problem is well-posed. The derivation of these conditions has been an important theme in this literature. (The whole question of compatibility becomes irrelevant, of course, when the surface-driven solution is used as the basis of the analysis.) The thermal parameters have been expressed most commonly as the solution of an integral equation, but the most general case considered so far has allowed only one of the two parameters to be an unknown function of temperature, the other being an

unknown constant. Because these solutions are very different in form from the expressions given in this paper, and because the geometry considered was planar (either slab or semi-infinite medium) rather than spherical, no attempt has been made to compare the results of this paper with the previously derived expressions for the thermal parameters.

1.1 Notation

The main analysis involves dimensionless quantities, which are designated by bare letters, whereas the corresponding dimensional quantities are indicated by an asterisk. Time-independent unit quantities (also dimensional) are indicated by a caret. The relations existing among the three types of quantities are given in table I which also serves to define most of the notation. (A few more symbols will be introduced as needed.) Table I also shows how the various dimensional quantities depend on the radius of the sphere. Because of thermal expansion, both the dimensional radius R^* and the dimensionless radius R are variable, but the unit radius $\hat{R}$ is an arbitrarily chosen constant. The R-dependence of the various dimensionless quantities has been defined in

TABLE I. *Basic Notation for Calorimetric Problem*.

Quantity	Dimensionless Symbol	Dimensional Symbol	Remarks
Radius of sphere	$R(t)$	$R^* = R\hat{R}$	
Radial distance	r	$r^* = rR\hat{R}$	$0 \leqslant r \leqslant 1$
Gradient operator	∇	$\nabla^* = R\hat{R}\,\nabla$	
Mass density	$\varrho(t)$	$\varrho^* = \varrho\hat{\varrho}/R^3$	$\begin{cases} \varrho \overset{\cdot}{=} \text{constant} \\ \nabla^*\varrho^* \overset{\cdot}{=} 0 \end{cases}$
Specific heat	$c(\Theta)$	$c^* = c\hat{c}$	$\begin{cases} k^* = \varrho^*\alpha^*c^* \\ \hat{k} = \hat{\varrho}\hat{\alpha}\hat{c} \\ k = \varrho\alpha c \end{cases}$
Thermal conductivity	$k(\Theta)$	$k^* = (k/R)\hat{k}$	
Thermal diffusivity	$\alpha(\Theta)$	$\alpha^* = R^2\alpha\hat{\alpha}$	
Total hemispherical emissivity	$\varepsilon(T)$	$\varepsilon^* = \varepsilon\hat{\varepsilon}$	
Linear time	t	$t^* = t\hat{t}$	$\hat{t} \equiv \hat{R}^2/\hat{\alpha}$
Nonlinear time	$\tau(t)$	$d\tau = \alpha(T)dt = \alpha^*dt^*/R^{*2}$	
Surface temperature	$T(t)$	$T^* = T\hat{T}$	
Interior temperature	$\Theta(t,r)$	$\Theta^* = \Theta\hat{T}$	$(\Theta)_{r=1} = T$
Surface specific enthalpy	$h(t)$	$h^* = h\hat{h}$	$\hat{h} \equiv \hat{c}\hat{T}$
Interior specific enthalpy	$\eta(t,r)$	$\eta^* = \eta\hat{h}$	$(\eta)_{r=1} = h$
Total mass		$M^* = \frac{4\pi}{3}R^{*3}\varrho^* = (\frac{4\pi}{3}\hat{R}^3\hat{\varrho})\varrho = \hat{M}\varrho$	
Total enthalpy (average specific enthalpy)	H	$H^* = M^*\eta_{av}\hat{h} = (\hat{M}\hat{c}\hat{T})\varrho H$	$H \equiv \eta_{av}$

Independent Reference Quantities: $\hat{R}, \hat{\varrho}, \hat{T}, \hat{c}, \hat{\alpha}$ (all constant)

such a way that the dimensionless Fourier equation is completely independent of the effects of thermal expansion. (Cf. Sec. 2.) During an observational run, $R^*(t^*)$ can be measured optically along with $T^*(t^*)$, and then $R(T^*)$ can be calculated. When, for example, this $R(T^*)$ is entered into the expression given in table I for α^*, the contribution to the T^*-dependence of α^* that results from thermal expansion is automatically taken into account. Throughout the paper, except for section 3 that deals with the predictive problem, it will be assumed that $R^*(t^*)$, $T^*(t^*)$, and dH^*/dt^* are given functions of t^* resulting from the experimental observations. From these the dimensionless functions $R(t)$, $T(t)$, and $\dot{H}(t) \equiv dH/dt$ can be directly calculated, so it will be assumed that these too are given functions. An overhead dot will indicate differentiation with respect to the dimensionless *linear* time t. It should usually be possible to choose the unit time $\hat{t}$ to be a convenient multiple of some experimentally defined time interval, such as the interval between observational readings. Differentiation with respect to the *nonlinear* time coordinate τ will be designated as follows: $dh/d\tau \equiv H^{(1)}$. Although it will often be desirable to choose $\hat{\varrho}$, $\hat{\alpha}$, and $\hat{c}$ to be close to the values of ϱ^*, α^*, and c^* at $T^* = \hat{T}$ (which means that the corresponding dimensionless quantities will be close to unity at the reference temperature $\hat{T}$), this is not necessary.

2. Surface-Driven Solution

If the spherical sample is imagined to be immersed in a heat reservoir of variable temperature, then changes in the interior temperature field are driven by the prescribed changes in the surface temperature. Assuming the absence of any interior heat sources, it follows that the interior temperature field is uniquely determined by the past history of the surface temperature up to the present moment. In mathematical terms, this corresponds to the "particular" or "driven" solution of the Fourier equation, with the surface temperature playing the role of the "driving function." This is not the most general solution, because it does not include the homogeneous solution which describes the decay of an arbitrarily specified initial interior temperature field. It is well known that the most slowly decaying term in the homogeneous solution has a time dependence proportional to $\exp(-\pi^2 t)$ where t is the dimensionless time measured in the natural time unit defined in table I. Neglecting the homogeneous solution amounts to assuming that the interior temperature field has been subjected to no influences other than its external environment for a period of time t that is long enough so that $\exp(-\pi^2 t) \ll 1$.

The time-rate at which the sample exchanges energy with its surroundings is determined by the history of the surface temperature up to the present moment. In fact, it is just equal to the time derivative of the total interior enthalpy of the sample. Thus, once the time history of the surface temperature has been specified, the time-rate of energy loss or gain of the sample is completely determined. The analysis of this section leads to expressions (summarized in tables V & VI) relating the time-rate of total energy change of the sample to the surface temperature (or more exactly, the specific enthalpy at the surface), and these expressions suffice for the analysis of both the predictive and the calorimetric problems.

The dimensional Fourier equation is given in the two forms (1a) and (1b) of table II, the only difference being the representation of the part of the heat flux that results from radial motion caused by thermal expansion or contraction. In eq (1a) it is represented in terms of the material velocity v^* at a point r^* that is fixed in the laboratory (inertial) frame, whereas in eq (1b) the motion is taken into account by the fact that the time derivative is taken with respect to fixed r rather than fixed r^*, where r is the dimensionless radial vector that is attached to a particular material particle and moves with it. Although v^*, which is the material velocity associated with thermal expansion or contraction, is negligibly small, the point to be made is that the right-hand side of the dimensionless Fourier equation given in eq (2) is rigorously correct, and the fact that the time derivative is taken at constant r rather than r^* does not represent an approximation.

In eq (3) the internal enthalpy density η is introduced in order to replace the internal temperature Θ. This replacement is doubly advantageous: First, a comparison of eqs (2) and (4) shows that it reduces the number of thermal parameters that appear in the equation. Second, the enthalpy density is really the quantity of physical interest, because the objective of the analysis is to integrate it over the volume of the sample in order to arrive at an expression for the time-rate of change of the total enthalpy (heat content) of the sample.

Equation (4a) still contains the temperature-dependent diffusivity $\alpha(\Theta)$, and this fact not only complicates the equation, but also prevents it from being universal in the sense of having the same form regardless of the material properties of the sample. If the diffusivity were a function only of t and not of r, it could be eliminated from the equation by replacing the linear dimensionless time t with the dimensionless nonlinear time τ as indicated in eq (5b). In fact, this device for eliminating the diffusivity has been used before [5,6]. The same device would also eliminate α from the equation if it were a function of the surface temperature $T(t)$

TABLE II. *Basic Differential Equation.*

Eq. No.

(1a,b) $\nabla^* \cdot (k^* \nabla^* \Theta^*) = \varrho^* c^* [\partial \Theta^* / \partial t^*]_{r^*} + v^* \cdot \nabla^* \Theta^*] = \varrho^* c^* (\partial \Theta^* / \partial t^*)_r$

(2) $\nabla \cdot (k \nabla \Theta) = \varrho c (\partial \Theta / \partial t)_r$

(3) $d\eta = c(\Theta) d\Theta$

(4a,b,c) $\nabla \cdot (\alpha \nabla \eta) = (\partial \eta / \partial t)_r; \quad \alpha = k / \varrho c; \quad \varrho \doteq \text{constant}$

(5a,b) $\nabla^2 \eta + \nabla \cdot u = (\partial \eta / \partial \tau)_r \; ; \quad d\tau \equiv \alpha(T[t]) dt = \alpha(t) dt$

(6a,b) $u \equiv -[1 - \dfrac{\alpha(\Theta)}{\alpha(T)}] \nabla \eta \; ; \quad \nabla \cdot u \equiv q_{eff}$

(7) $\dfrac{\partial^2 (r\eta)}{\partial r^2} - \dfrac{\partial (r\eta)}{\partial \tau} = -r q_{eff} = \dfrac{1}{r} \dfrac{\partial}{\partial r} \{ [1 - \dfrac{\alpha(\Theta)}{\alpha(T)}] r^2 \dfrac{\partial \eta}{\partial r} \} \doteq 0$

(8a,b) $[\eta(r,\tau)]_{r=1} = h(\tau) \; ; \quad \left(\dfrac{\partial \eta}{\partial r} \right)_{r=1} = \dfrac{1}{3} \dfrac{dH}{d\tau} \equiv \dfrac{1}{3} H^{(1)}$

(8c) $H \equiv \eta_{av} = \int_0^1 \varrho \eta r^2 dr / \int_0^1 \varrho r^2 dr = 3 \int_0^1 \eta r^2 dr$

rather than of the interior temperature $\Theta(r,t)$. Even in the latter case, however, introduction of a nonlinear time τ based on $\alpha(T[t])$ succeeds in eliminating most of the α-dependence from the equation, as shown by eqs (5a) and (6a). What remains in the equation is a very small effective heat source density term q_{eff} which has the form of the divergence of an effective heat flux u defined in eq (6a). This heat flux vanishes at the surface of the sample, and for this reason, when Gauss' theorem is applied to eq (5a) in order to arrive at the expression given in eq (8b) for the time-rate of total enthalpy change, the term involving u makes no contribution. Therefore, because eq (8b) leads to the equation (eq (19) of table V) from which the rest of the analysis follows, it is evident that, at least to first order, the introduction of the nonlinear time τ has succeeded in reducing the problem to the solution of the universal equation that results if $q_{eff} = 0$ in eq (7). The analysis of this paper is based on this approximation. If more accuracy should be required, then the solution for $\eta(r,\tau)$ that is given in eq (9) or eq (12) of table III could be substituted into the right-hand side of eq (7), and an additive correction to η could be found which in turn would lead to an additive correction to H which could be introduced into the calorimetric equations of section 4. The way this would be done is explained in section 5.

The solution to eq (7) (with 0 on the right-hand side) that satisfies the boundary condition stated in eq (8a) can be written in the form of eq (9) in table III. The polynomials $p_n (r)$ are characterized by the property stated in eq (10a), and can be generated by successive integration. The first four polynomials are given in eq (11), and are plotted in figure 1. The fact that eq (9) does indeed satisfy eq (7) (with 0 on the right-hand side) can be directly confirmed using the property stated in eq (10a).

As indicated in eq (12), the solution can also be expressed in terms of the odd-order Bernoulli polynomials $B_{2n+1}(x)$ where $x = \frac{1}{2}(1-r)$. The properties of these polynomials that are necessary to verify that eq (12) is indeed the desired solution of eq (7) are stated in eqs (13) and (14). (See for example, pp. 804-811 of Ref. [14] or pp. 19, 25-29 of Ref. [15].)

An explicit expression for $H^{(1)} \equiv dH/d\tau$ in terms of $h^{(n)} \equiv d^n h/d\tau^n$ can be derived by substituting eq (12) into the left-hand side of eq (8b) and using the relation stated in eq (16) of table IV between the even-order Bernoulli numbers B_{2n} and the Riemann Zeta function $\zeta(2n)$. The resulting relation is given in eq (19) of table V. Using the numerical values for $\zeta(2n)$ that are given in table IV, eq (20) results, which can be then inverted to yield eq (21), which will play an important role in section 4.

The expansion given in eq (19) assumes that $h(\tau)$ is an analytic function all of whose derivatives exist. If in addition it remains finite for all τ, it can be shown that eq (19) is equivalent to the integral equation given in eqs

517

TABLE III. *Surface-Driven Solution for Interior Enthalpy Density.*

Eq. No	
(9a,b)	$\eta(r,\tau) = h(\tau) + \sum_{n=1}^{\infty} (-1)^n p_n(r) h^{(n)}(\tau)$; $h^{(n)} \equiv d^n h/d\tau^n$
(10a,b)	$d^2(rp_n)/dr^2 = -rp_{n-1}$ or $\nabla^2 p_n = -p_{n-1}$
(11a)	$p_1 = (1-r^2)/6$
(11b)	$p_2 = (7 - 10r^2 + 3r^4)/360$
(11c)	$p_3 = (31 - 49r^2 + 21r^4 - 3r^6)/15{,}120$
(11d)	$p_4 = (381 - 620r^2 + 294r^4 - 60r^6 + 5r^8)/1{,}814{,}400$

Cf. Fig. 1

(12a,b)	$\eta(r,\tau) = h(\tau) - \frac{1}{r} \sum_{n=1}^{\infty} \frac{2^{2n+1}}{(2n+1)!} B_{2n+1}(x) h^{(n)}(\tau)$; $x \equiv \frac{1}{2}(1-r)$
(13a,b)	$[B_{2n+1}(x)]_{r=0} = B_{2n+1}(\frac{1}{2}) = 0$; $[B_{2n+1}(x)]_{r=1} = B_{2n+1}(0) = 0$
(14a,b)	$\dfrac{dB_{2n+1}(x)}{dr} = -\frac{1}{2}(2n+1)B_{2n}(x)$; $\dfrac{d^2 B_{2n+1}(x)}{dr^2} = \frac{1}{4}(2n+1)(2n)B_{2n-1}(x)$

(22a) and (23) of table VI. The kernel Γ of the convolution integral defined in eq (23) is an effective memory function that weights the very recent past most heavily and totally forgets events that happened more than half a natural time unit in the past. This memory function is defined by eq (24) and is plotted in figure 2. Its argument is defined by eq (27a), and as shown in eqs (27b and c) can be expressed in terms of $\alpha(t)$ and the difference $(t-t')$ between the present time t and some past time t'. Figure 2 shows that for ζ less than 0.1 natural time units the simple function $\tilde{\Gamma}$ defined by eq (25b) is essentially indistinguishable from Γ. For larger ζ, the first term in the summation of eq (24) should serve to represent Γ with sufficient accuracy for most purposes. As eq (26) indicates, the normalization of Γ is such that if $h^{(2)}$ is constant, then the retrospective weighted average $\overline{h^{(2)}}$ defined by eq (23) will just be equal to $h^{(2)}$. If, however, $h^{(2)}$ varies drastically during half a natural time unit, which could be the case when a sample first starts to cool, then the weighted average $\overline{h^{(2)}(t)}$ will differ markedly from the instantaneous value $h^{(2)}(t)$. In such a case the integral eq (22a) will be more accurate than the equivalent truncated expansion given in eq (20). The series expansion (19) can be derived from the integral equation defined by eqs (22a) and (23b) by expressing $h^{(2)}(\tau - \zeta)$ as a Taylor expansion about τ, integrating by parts, and making use of the definition of $\zeta(2n)$ given in

eq (15) in table IV.

Finally, it should be noted that it is evident from eq (23b) that when $\overline{h^{(2)}(\tau)}$ is differentiated with respect to τ, the differentiation can be taken inside the integration, from which it follows that eq (22b) results from differentiation of eq (22a). Obviously, an infinity of such equations can be generated by repeated differentiation.

TABLE IV. *Riemann Zeta Function for Even-Integer Argument.*

Eq. No.	
(15)	$\zeta(2n) \equiv \sum_{m=1}^{\infty} m^{-2n}$
(16)	$B_{2n} \equiv [B_{2n}(x)]_{x=0} = \dfrac{(-1)^{n-1}(2n)!}{2^{2n-1}} \dfrac{\zeta(2n)}{\pi^{2n}}$

$2n$	$\zeta(2n)/\pi^{2n}$	$\zeta(2n)$
2	1/6	1.64493
4	1/90	1.08232
6	1/945	1.01734
8	1/9450	1.00407
10	1/93,555	1.00099

TABLE V. *Total Rate of Energy Loss: Differential Representation.*

Eq. No.	
(17a,b,c)	$H^{(1)} \equiv dH/d\tau$; $\quad \dot{H} \equiv dH/dt$; $\quad H^{(1)} = \dot{H}/\alpha(t)$
(18a,b)	$h^{(1)} = c(\tau)T^{(1)}(\tau) = c(t)\dot{T}(t)/\alpha(t)$; $\quad h^{(n)} \equiv d^n h/d\tau^n$
(19)	$H^{(1)}(\tau) = -6 \sum\limits_{n=1}^{\infty} (-1)^n [\zeta(2n)/\pi^{2n}]\, h^{(n)}(\tau)$
(20)	$H^{(1)}(\tau) = h^{(1)} - \frac{1}{15} h^{(2)} + \frac{2}{315} h^{(3)} - \frac{1}{1575} h^{(4)} + \dots$
(21)	$h^{(1)}(\tau) = H^{(1)} + \frac{1}{15} H^{(2)} - \frac{1}{525} H^{(3)} + \frac{2}{23,625} H^{(4)} + \dots$

TABLE VI. *Total Rate of Energy Loss: Integral Representation.*

Eq. No.	
(22a,b)	$H^{(1)} = h^{(1)} - \frac{1}{15} \overline{h^{(2)}}$; $\quad H^{(2)} = h^{(2)} - \frac{1}{15} \overline{h^{(3)}}$; etc.
(23a,b)	$\overline{h^{(2)}} \equiv \int_{-\infty}^{\tau} \Gamma(\tau-\tau')\, h^{(2)}(\tau')d\tau' = \int_0^{\infty} \Gamma(\zeta)\, h^{(2)}(\tau-\zeta)d\zeta$
(24)	$\Gamma(\zeta) \equiv 90 \sum\limits_{m=1}^{\infty} (m\pi)^{-2} \exp[-(m\pi)^2\zeta]$
(25a)	$\Gamma(\zeta) \doteq \tilde{\Gamma}(\zeta)$ for $0 \leqslant \zeta \leqslant 0.1$
(25b)	$\tilde{\Gamma}(\zeta) \equiv 15[1-3(2\sqrt{\zeta/\pi} - \zeta)]$
(26a,b)	$\int_{-\infty}^{\tau} \Gamma(\tau-\tau')d\tau' = \int_0^{\infty} \Gamma(\zeta)d\zeta = 1$
(27a)	$\zeta \equiv \tau-\tau' = \int_{t'}^{t} \alpha(t'')dt''$
(27b)	$\zeta(\alpha;\ t-t') = \sum\limits_{n=0}^{\infty} \frac{(-1)^n}{(n+1)!} (d^n\alpha/dt^n)(t-t')^n$
(27c)	$\zeta(\alpha;\ t-t') = \dot{\alpha}(t)(t-t') - \frac{1}{2}\ddot{\alpha}(t)(t-t')^2 + \frac{1}{6}\dddot{\alpha}(t)(t-t')^3 - \dots$

Equations (24), (25a), (25b): (Cf. Fig. 2)

3. The Predictive Problem

For the purpose of estimating radiative cooling times and the relative magnitudes of the terms in eq (21), from which the calorimetric equations of section 4 are derived, it is useful to solve the post-transient predictive problem for the case of constant parameters. In such a case the simplifications indicated in eqs (28a-d) of table VII occur. All of the equations of tables V and VI are still valid. In particular, $\dot{H} = H^{(1)}$ must satisfy eq (19), but in addi-

tion it must satisfy the Stefan-Boltzmann radiation law which means that the left-hand side of eq (19) must be replaced by T^4 multiplied by a proportionality constant involving the Stefan-Boltzmann constant $\sigma^* = \hat{\sigma}$. It is easy to show that if the unit temperature $\hat{T}$ is defined as shown in eq (29b), the proportionality constant on the left side of the specialized form of eq (19) will by unity, with the result that the equation has the form given in eq (31). A significant feature of this equation is that it is universal in the sense that it applies to spherical samples of all sizes made of any material whose thermal
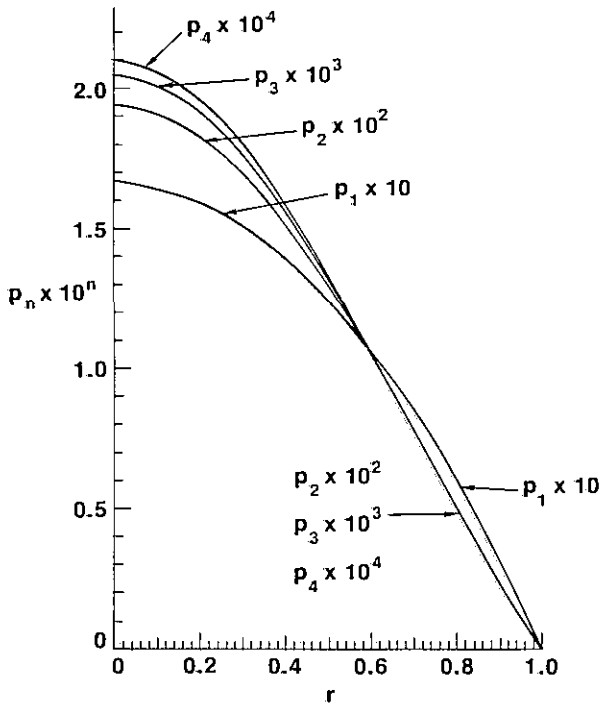
FIGURE 1. Dimensionless polynomials $p_n(r)$ defined in eqs (11a-d).
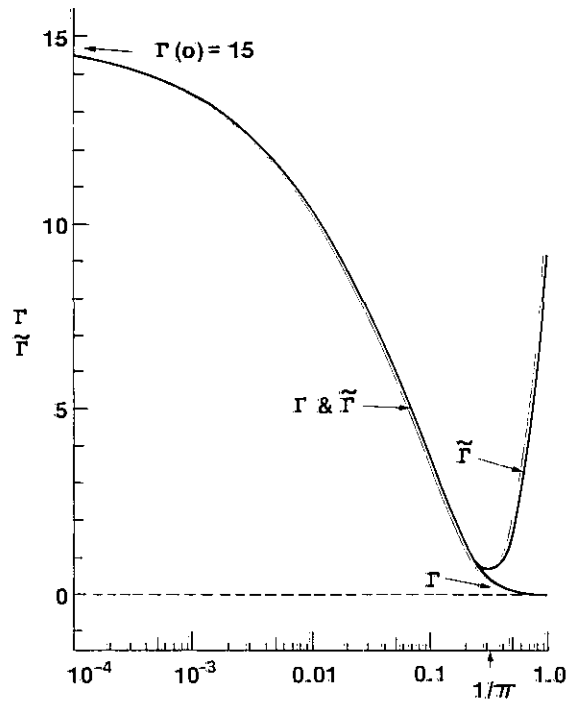
FIGURE 2. Dimensionless kernel $\Gamma(\zeta)$ in convolution integral defined in eq (23), and approximate kernal $\tilde{\Gamma}(\zeta)$ defined in eq (25b), both as functions of the dimensionless argument $\zeta \equiv \tau - \tau'$.

TABLE VII. *Equations for Predictive Problem.*

Eq. No.	
(28a,b,c,d)	$c = \alpha = k = R = \varepsilon = \varrho = 1;\ \tau = t;\ \eta = \Theta;\ h = T$
(29a,b)	$T = T^*/\hat{T};\ \hat{T} \equiv (\hat{k}/\hat{R}\hat{\sigma}\hat{\varepsilon})^{1/3} = (k^*/R^*\sigma^*\varepsilon^*)^{1/3} = (\varrho^*\alpha^*c^*/R^*\sigma^*\varepsilon^*)^{1/3}$
(30a,b)	$\dot{H} \equiv dH/dt = -3T^4;\ (\partial\eta/\partial r)_{r=1} = (\partial\theta/\partial r)_{r=1} = -T^4$
(31)	$T^4 = 2\sum_{n=1}^{\infty} (-1)^n [\zeta(2n)/\pi^{2n}]d^n T/dt^n$
(32)	$T^4 = -\frac{1}{3}\frac{dT}{dt} + \frac{1}{45}\frac{d^2T}{dt^2} - \frac{2}{945}\frac{d^3T}{dt^3} + \frac{1}{4725}\frac{d^4T}{dt^4} - \cdots$
(33a,b)	$dT/dt = -3T^4[1 - \frac{4}{5}T^3 + \frac{4}{25}T^6 + \frac{144}{875}T^9 + \ldots];\ dH/dt = -3T^4$
(34a,b)	$d^2T/dt^2 = 36\ T^7\ [1 - \frac{11}{5}T^3 + \frac{42}{25}T^6 + \ldots]\quad;\ d^2H/dt^2 = 36T^7\ [1 - \frac{4}{5}T^3 + \frac{4}{25}T^6 + \ldots]$
(35a,b)	$d^3T/dt^3 = -756\ T^{10}\ [1 - \frac{138}{35}\ T^3 + \ldots]\quad;\ d^3H/dt^3 = -756T^{10}\ [1 - \frac{68}{35}\ T^3 + \ldots]$
(36a,b)	$d^4T/dt^4 = 22{,}680\ T^{13} - \ldots\quad;\ d^4H/dt^4 = 22{,}680\ T^{13} - \ldots$
(37)	$t(T) \doteq \frac{1}{9}(T^{-3} - 1) - \frac{4}{15}\ln T + \frac{4}{75}(1 - T^3)$
(38)	$T(t) \doteq [(1 + 9t) - \frac{4}{15}\ln(1 + 9t) - \frac{108}{25}\frac{1}{(1 + 9t)}]^{-1/3}$
(39)	$T(t) = [-\frac{1}{3}\dot{T}(t) + \frac{1}{45}\int_0^\infty \Gamma(\zeta)\ddot{T}(t-\zeta)d\zeta]^{1/4}$

(Cf. Fig. 3)

parameters are constants. It is possible to solve this equation by truncating it at the fourth derivative as shown in eq (32), and solving the truncated equation for dT/dt in terms of T by starting with the approximation $dT/dt \doteq -3T^4$ and iterating until a self-consistent set of expressions for the first four derivatives results. These expressions are given in eqs (33a-36a). By differentiating eq (30a) and making use of eqs (33a-36a), the expressions for d^nH/dt^n given in eqs (34b-36b) can be derived. The 8 expressions in eqs (33-36) will be used in section 4 to estimate the range of validity of the calorimetric formulas derived there. Numerical estimates indicate that these expressions are accurate to within 1% so long as $T \leqslant \frac{1}{2}$. For larger T, it would be necessary to include higher order terms in the expansion given in eq (31), and the numerical estimates indicate that for $T > 3/4$ the convergence is so slow that this expansion has no practical utility. Correspondingly, the calorimetric equations derived in section 4 that are based on eq (21), which is derived from eq (19), cannot be expected to be accurate, even in a post-transient experiment, if the dimensionless surface temperature T based on the unit temperature defined in eq (29b) is larger than $\frac{1}{2}$. If the sphere size and thermal parameters are such that $T > \frac{1}{2}$, then it will be necessary to use equations based on the integral equation defined by eqs (22a) and (23). In order to give a feeling for what sphere sizes and which materials will satisfy the condition $T < \frac{1}{2}$, the dimensionless temperatures T_{melting} corresponding to the respective melting points of tungsten (3650 K) and uranium dioxide (3150 K) are given in table VIII for sphere radii that approximate the upper and lower limits that would most probably be considered for radiative-cooling calorimetry experiments. It is evident from this chart that for most practical post-transient experiments, it should be possible to use calorimetric relations derived from the truncated expansion given in eq (21). Only in the case of a large sample $(\hat{R} \approx 1 \text{ cm})$ of a poor thermal conductor (such as uranium dioxide) might it be necessary to use an integral relation in order to analyze the results of a post-transient experi-

FIGURE 3. Universal temperature-time curve for post-transient radiative cooling.

ment. It ought to be noted, however, that this might be necessary even in the case of a smaller sample of a better conductor if the observations are based on a transient-type experiment.

A universal post-transient cooling curve can be derived by integrating eq (33a). The result is the expression for $t(T)$ given in eq (37). This can be inverted to yield the expression for $T(t)$ given in eq (38). The cooling curve corresponding to these expressions is plotted in figure 3. It is evident from this curve that the slope of $\ln T$ versus $\ln t$ is almost, but not quite, constant. In fact, this slight variation in slope is related to the thermal conductivity of the sample. It can be shown that for initial and final temperatures T_i^* and T_f^*

$$k^* = \frac{4}{15} \hat{R}\hat{\sigma}\hat{\varepsilon} \left(\frac{T_i^{*3} - T_f^{*3}}{s_i - s_f} \right) \quad (40 \text{ a})$$

$$s_i = \left(\frac{d \ln T^*}{d \ln t^*} \right)_{T_i^*} \; ; \; s_f = \left(\frac{d \ln T^*}{d \ln t^*} \right)_{T_f^*} \quad (40 \text{ b,c})$$

This equation cannot be used for determining thermal conductivity from observation of post-transient radiative cooling, because it assumes that the specific heat is constant throughout the cooling, whereas in all probability the $\ln T^*$ versus $\ln t^*$ curve for a real sample would have much more curvature than the one shown in figure 3, and most of this curvature would be caused by the temperature dependence of the specific heat. The real significance of eq (40) is that it (together with Fig. 3) illustrates how difficult it is to make a reliable determination of thermal conductivity (or diffusivity) from observations of post-transient radiative cooling,

TABLE VIII. *Representative Values for Unit Time and Unit Temperature.*

$\hat{R}$	Tungsten		Uranium Dioxide	
	0.1 cm	1 cm	0.1 cm	1 cm
$\hat{t}$	0.03 sec	3 sec	2 sec	200 sec
$\hat{T}$	37,000 K	17,000 K	8100 K	3800 K
T^*_{melting}	3650 K	3650 K	3150 K	3150 K
T_{melting}	0.1	0.2	0.4	0.8

$\hat{t} = \hat{R}^2/\hat{\alpha}; \quad \hat{T} = (\hat{k}/\hat{R}\hat{\sigma}\hat{\varepsilon})^{1/3} = (\hat{\rho}\hat{\alpha}\hat{c}/\hat{R}\hat{\sigma}\hat{\varepsilon})^{1/3}$

especially when these observations are made for temperatures near the lower end of the curve shown in figure 3. In contrast, it is very easy to determine the specific heat in this range since to a good approximation it will be given by $c = \dot{H}/\dot{T}$. For an accurate determination of thermal conductivity it will probably be necessary to use a sphere that is large enough so that the dimensionless temperatures involved fall well above those shown in figure 3. In such a case it would be necessary to analyze the data using the integral expressions given in section 4, rather than the truncated expansions.

It should be noted that when the expressions given in eqs (33a-36a) are substituted into eq (9a) taking the simplifications stated in eqs (28a-d) into account, a complete solution for the interior surface-driven solution in terms of the surface temperature T results. If the expression for $T(t)$ given in eq (38) is substituted into this, an explicit expression for the interior temperature field $\Theta(r,t)$ results. If it were desired to extend the validity of this solution to values of T larger than $\frac{1}{2}$, this could be done by using the integral equation given in eq (39) in table VII as the basis for an iterative solution. Equation (39) was derived from the integral equation defined by eqs (22a) and (23), making use of eq (30a). The idea of reducing the problem of solving for the interior temperature field to the problem of solving an integral equation involving only the time dependence of the surface temperature is not new. It has been done for a semi-infinite medium with a plane surface [16]. The integral equation that resulted was derived from the diffusion convolution integral mentioned in section 1. However, this approach is not appropriate for the present problem because, as noted in section 1, the diffusion convolution integral represents the temperature field in an infinite medium surrounding a spherical cavity, rather than the field within a finite spherical medium.

4. The Calorimetric Problem

In adapting the expressions derived in section 2 to the problem of deducing the specific heat and the thermal diffusivity from observational data, the choice made for the unit temperature $\hat{T}$ can be arbitrary. It is not necessary to use the unit temperature defined by eq (29b) of table VII, although this choice is appropriate for the purposes of designing an experiment, and for determining whether the various expressions derived in section 4.1 from eq (21) are accurate, or whether it is necessary to use the alternative integral relations discussed in section 4.2.

Once it is a question of analyzing existing data, however, it would generally be more convenient to define

$\hat{T}$ so that the dimensionless temperature T is close to unity. If the thermal parameters are already known for the cold end of a post-transient cooling run, then it would be natural to choose this cold temperature as the unit temperature, and correspondingly the unit specific heat and unit diffusivity would be chosen to be equal to the known values of these parameters at this cold temperature. If the true values are not known, then estimates would suffice. Nowhere in the analysis is it assumed that these estimates are close to the true values. For example, if one were analyzing data for samples of different materials, it might be most convenient to make a single choice of unit quantities to be used for all of the different materials.

In all of the expressions given below, $\dot{H}(t) \equiv dH/dt$ and $T(t)$ are regarded as given functions of time that result from independent simultaneous observations made by two different instruments. If a reliable cooling law exists and is known, then $\dot{H}$ can be expressed as a function of T and eliminated from the equations. In the case of radiative cooling, this would require that the temperature dependence of the total hemispherical emissivity $\varepsilon(T)$ be known.

4.1 Truncated Expansions

The calorimetric formulas, which were the principal objective of this analysis, are given in eqs (41) and (42) of table IX. The expression for c follows directly from eq (40), which is simply eq (21) of table V multiplied by $\alpha(t)$. The expression for α was derived from the ratio of the time derivative of eq (40a) to eq (40a) itself. Both expressions for c and α have the form of a power series in an expansion parameter $\xi = 1/15\alpha$. The coefficients of these power series are functions of the four quantities defined in eqs (43a-d), the leading terms of which are ratios of different time derivatives of T and H. Equations (44) and (45) give approximate expressions for c and α that are valid in the limiting case in which only the leading terms in the expansions must be retained, and c and α *are essentially constant.*

In the discussion that follows, it will be assumed that the unit of diffusivity $\hat{\alpha}$ has been chosen so that for the data under consideration the dimensionless diffusivity α is of order unity. Then $\xi \approx 1/15$. (If a different choice of $\hat{\alpha}$ were made, the change in ξ would be compensated by changes in the values of the quantities defined in eqs (43a-d).) Because the expansion parameter ξ involves α, and the coefficients in the expansions for c and α involve $\dot{c}$ and $\dot{\alpha}$, it is evident that eqs (41) and (42) must be solved iteratively, with the first iteration based on the assumption that $\xi = \dot{c} = \dot{\alpha} = 0$. The range of convergence of this procedure can be estimated by using the

expressions for d^nT/dt^n and d^nH/dt^n given in eqs (33-36) of table VII to evaluate all of the terms in eqs (41) and (42). When this is done the following expressions result:

$$A = -12\,T^3\left(1 - \frac{7}{5}T^3 + \frac{2}{5}T^6 + \ldots\right) \qquad (46a)$$

$$B = -12\,T^3\left(1 - \frac{4}{5}T^3 + \frac{4}{25}T^6 + \ldots\right) \qquad (46b)$$

$$C = 252\,T^6\left(1 - \frac{68}{35}T^3 + \ldots\right) \qquad (46c)$$

$$D = -7560\,T^9 + \ldots \qquad (46d)$$

$$\frac{D - AC}{A - B} = -630\,T^3 + \ldots \qquad (47a)$$

$$\frac{AD}{A - B} = 12{,}600\,T^6 + \ldots \qquad (47b)$$

$$c_o = \dot{H}/\dot{T} = 1 + \frac{4}{5}T^3 + \frac{12}{25}T^6 \qquad (48)$$

$$+ \frac{16}{175}T^9 + \ldots$$

$$\alpha_o = \frac{1}{15}\left(\frac{C - AB}{A - B}\right) = 1 - \frac{6}{5}T^3 + \ldots \quad . \qquad (49)$$

When these expressions and $\xi \approx 1/15$ are substituted into the right-hand side of eq (41a), it reduces to $1 + 0(T^{12})$ which (since the left-hand side is $c = 1$) is just the identity that is to be expected in view of the fact that eq (41a) is simply a reformulation of the same equation from which eqs (33-36) were derived. Similarly, the right-hand side of eq (42) reduces to $1 + 0(T^6)$. Thus (to the accuracy of the truncation) the leading factors in eqs (41a) and (42), which are now expressed by eqs (48) and (49), are just the reciprocals of the respective square brackets on the right-hand sides of eqs (41a) and (42). For this reason, the speed of convergence of the calorimetric formulas can be estimated by inspecting eqs (48) and (49). These indicate acceptably rapid convergence for $T < \frac{1}{2}$ which, of course, is the same range of convergence that was noted in section 3 for the validity of the iterative solution of the predictive problem.

In the case of the approximate limiting expressions given in eqs (44) and (45), all of the terms of eqs (41a) and (42) that involve ξ were thrown away, and only the leading terms were retained. In addition, all of the terms of eqs (43a-d) involving $\dot{c}$ and $\dot{\alpha}$ were thrown away. The validity of this latter approximation can be answered only on a case-by-case basis, but the validity of ignoring the terms involving ξ can be estimated by means of eqs (48) and (49) since the terms involving T represent the error in these formulas, because in this case the correct values of c and α are unity. In the chart below the magnitudes of the two leading error terms are listed for several values of T.

T	$\frac{4}{5}T^3$	$\frac{6}{5}T^3$
½	0.10	0.15
¼	0.013	0.019
0.1	0.0008	0.001

This chart shows that for $T < \frac{1}{4}$, the error is less than 2 percent, and becomes increasingly smaller the smaller T becomes, i.e, as T enters the extreme post-transient regime. Even for $T = \frac{1}{2}$, the error is not so large as to destroy the usefulness of eqs (44) and (45) for generating the first iterative solution for $c(t)$ and $\alpha(t)$ which is then substituted into the right-hand sides of the more accurate formulas given in eqs (41) and (42). If α_0 is constant, it follows from eq (45d) that $\dot{H} \propto \exp[-15\alpha_0 t]$, so that in the extreme post-transient regime α_0 can be estimated by fitting the observed function $\dot{H}(t)$ to an exponential decay.

It should be noted that, in order to make these estimates, it has been necessary to define the dimensionless T in the manner indicated in eq (29) of table VII. This automatically takes the sphere size and thermal parameters of the sample into account. However, for an actual application of the calorimetric formulas of table IX, it is not necessary to do this. One may use any convenient scaling factor to define the dimensionless T. The validity of the formulas would then be indicated directly by the convergence behavior of the numerical iteration process.

The solutions of eqs (41) and (42) are $c(t)$ and $\alpha(t)$. However, because $T(t)$ is known from observation, these solutions can be converted into $c(T)$ and $\alpha(T)$, which are the desired expressions for the temperature dependence of the thermal parameters.

4.2 Integral Relations

If a numerical application of the calorimetric formulas shows that the ξ^3 term in eq (42) is comparable in magnitude with the ξ^2 term, or if the ξ^2 term in eq (41a) is comparable with the ξ term, this is an indication that the neglected higher-order terms are not really negligible, and that the calculated functions $\alpha(t)$ and $c(t)$ are not reliable. One could, of course, include higher-order terms in the equations, but truncation must occur at some point, so the net result would be only a slight extension of the range of validity of the equations. Moreover, the higher-order terms involve higher derivatives of $T(t)$

TABLE IX. *Calorimetric Problem: Truncated Expansions.*

Eq. No.	

(40a,b) $\quad \dot{h} = c\dot{T} = \dot{H} + \frac{1}{15}[\frac{dH^{(1)}}{dt} - \frac{1}{35}\frac{dH^{(2)}}{dt} + \frac{2}{1575}\frac{dH^{(3)}}{dt} + \ldots];$

$\qquad [H^{(1)} = \frac{\dot{H}}{\alpha}, \; H^{(2)} = \frac{1}{\alpha}\frac{dH^{(1)}}{dt}, \; H^{(3)} = \frac{1}{\alpha}\frac{dH^{(2)}}{dt}]$

(41a,b) $\quad c = (\dot{H}/\dot{T})[1 + B\xi - (\frac{3}{7}C)\xi^2 + (\frac{2}{7}D)\xi^3 + \ldots]; \; \xi \equiv 1/15\alpha$

(42) $\quad \alpha = \frac{1}{15}(\frac{C-AB}{A-B})[1 - \frac{3}{7}(\frac{D-AC}{A-B})\xi^2 - \frac{2}{7}(\frac{AD}{A-B})\xi^3 + \ldots]$

(43a) $\quad A \equiv d\ln h^{(1)}/dt = d\ln(c\dot{T}/\alpha)/dt = (\ddot{T}/\dot{T}) + [(\dot{c}/c) - (\dot{\alpha}/\alpha)]$

(43b) $\quad B \equiv d\ln H^{(1)}/dt = d\ln(\dot{H}/\alpha)/dt = (\ddot{H}/\dot{H}) - (\dot{\alpha}/\alpha)$

(43c) $\quad C \equiv \alpha^2 H^{(3)}/H^{(1)} = (\dddot{H}/\dot{H}) - 3(\dot{\alpha}/\alpha) + [(\ddot{\alpha}/\alpha) + (\dot{\alpha}/\alpha)^2]$

(43d) $\quad D \equiv \alpha^3 H^{(4)}/H^{(1)} = (\ddddot{H}/\dot{H}) - 6(\dot{\alpha}/\alpha)(\dddot{H}/\dot{H}) + [15(\dot{\alpha}/\alpha)^2 - 4(\ddot{\alpha}/\alpha)](\ddot{H}/\dot{H}) - [(\dddot{\alpha}/\alpha) + 15(\dot{\alpha}/\alpha)^3$

$\qquad - 10(\dot{\alpha}\,\ddot{\alpha}/\alpha^2)]$

(44) $\quad c_0 \equiv (c)_{\xi=\dot{c}=\dot{\alpha}=0} = \dot{H}/\dot{T}$

(45a,b) $\quad \alpha_0 \equiv (\alpha)_{\xi=\dot{c}=\dot{\alpha}=0} = \frac{1}{15}(\frac{C-AB}{A-B})_{\dot{c}=\dot{\alpha}=0} = \frac{1}{15}\frac{(\dot{T}\,\dddot{H} - \dddot{T}\,\dot{H})}{(\ddot{T}\,\dot{H} - \dot{T}\,\ddot{H})}$

(45c,d) $\qquad = -\frac{1}{15}\begin{vmatrix} \dot{T} & \ddot{H} \\ \ddot{T} & \dddot{H} \end{vmatrix}\begin{vmatrix} \dot{T} & \dot{H} \\ \ddot{T} & \ddot{H} \end{vmatrix}^{-1} = -\frac{1}{15}\frac{d}{dt}(\frac{\ddot{H}}{\dot{T}}) / \frac{d}{dt}(\frac{\dot{H}}{\dot{T}})$

TABLE X. *Calorimetric Problem: Integral Relations.*

Eq. No.	

(50) $\quad \alpha(t) = \left\{ [(\ddot{h} - \ddot{H})/(\dot{h} - \dot{H})] - (\dot{\alpha}/\alpha) \right\} [\overline{h^{(2)}}/\overline{h^{(3)}}]$

(51) $\quad \dot{h}(t) = \dot{H} + \frac{1}{15}\left\{ [(\ddot{h} - \ddot{H})/(\dot{h} - \dot{H})] - (\dot{\alpha}/\alpha) \right\} [(\overline{h^{(2)}})^2/\overline{h^{(3)}}]$

(52) $\quad \overline{h^{(2)}} \equiv \int_{-\infty}^{\tau} \Gamma \frac{d}{dt'}[\frac{\dot{h}(t')}{\alpha(t')}]dt'$

(53) $\quad \overline{h^{(3)}} \equiv \int_{-\infty}^{t} \Gamma \frac{d}{dt'}\left\{ \frac{1}{\alpha(t')}\frac{d}{dt'}[\frac{\dot{h}(t')}{\alpha(t')}] \right\}dt'$

(54) $\quad \Gamma \equiv 90 \sum_{m=1}^{\infty} (m\pi)^{-2}\exp[-(m\pi)^2\xi]$

(55) $\quad \xi \equiv \int_{t'}^{t} \alpha(t'')dt'' = \alpha(t)(t-t') - \frac{1}{2}\dot{\alpha}(t)(t-t')^2 + \frac{1}{6}\ddot{\alpha}(t)(t-t')^3 - \ldots$

(56) $\quad c(t) = \dot{h}(t)/\dot{T}(t)$

(57a,b) $\quad c(T) = c(t[T]); \; \alpha(T) = \alpha(t[T])$

and $\dot{H}(t)$, and the error involved in extracting these from the experimental data becomes ever greater the higher the order of differentiation. For these reasons, it is better to use an iterative procedure based on eqs (50) and (51) of table X which involve the integrals defined in eqs (52) and (53). These equations were derived from eqs (22a) and (22b) of table VI. Because $\ddot{h}(t) = c(t)\,\ddot{T}(t)$, eq (51) is really an equation for $c(t)$, but it is simpler to regard $h(t)$ as the unknown function and, after this has been found, to invoke eq (56) to find $c(t)$, and eqs (57a,b) to find $c(T)$ and $\alpha(T)$. The kernel Γ of the integrals is defined by eqs (54) and (55), but the approximation based on eq (25b) and discussed at the end of section 2 would simplify the calculations. Inasmuch as the temperature dependence (and hence the time dependence) of α is usually weak, and (as Fig. 2 indicates) Γ will usually vanish in a time interval that is short compared with the time required for α to change by a significant amount, in all but the most extreme of transient experiments it would be justified to drop all but the first term in the expansion for ζ given in eq (55).

The iteration could be started with an $\alpha(t)$ calculated from eq (45) and an $\ddot{h}(t) = c(t)\,\ddot{T}(t)$ where $c(t)$ is found from eq (44). These approximate functions would be substituted into the right-hand sides of eqs (50) and (51), which would yield new (presumably improved) approximations. Questions of convergence and numerical stability of this procedure have not yet been investigated.

5. Discussion

The foregoing analysis took the temperature dependence of the specific heat fully into account, but the interior spatial variation of the diffusivity was neglected. This amounted to neglecting an effective heat source density in the Fourier equation, but it was pointed out in section 2 that this neglected term could be taken into account in an iterative fashion. This would give rise to an additive correction $\delta_\alpha\eta$ to the interior enthalpy density field. It was noted in section 2 that when Gauss' theorem is applied to the Fourier equation, the effective heat term makes no direct contribution to the resulting equation (eq (8b) in table II). It does make an indirect contribution, however, in the sense that it produces an additive correction to the radial derivative of the interior enthalpy field. Thus, eq (8b) must be replaced by

$$[\partial(\eta + \delta_\alpha\eta)/\partial r]_{r=1} = \tfrac{1}{3}d(H + \delta_\alpha H)/d\tau \quad (58a)$$

where H is given by eq (8c) and $\delta_\alpha H$ is given by

$$\delta_\alpha H = 3 \int_0^1 (\delta_\alpha\eta)r^2 dr \; . \quad (58b)$$

The total time-rate of energy loss of the sample, which is to be identified with the observed energy flux, is given by $\dot{H}_{\text{tot}} = \dot{H} + \delta_\alpha\dot{H}$. It is important to note that, in making the correction to the calorimetric formulas of section 4, $\dot{H}_{\text{tot}}$ must not be substituted in place of $\dot{H}$. The reason for this is that these formulas were all derived from eq (19) (or its integral equivalent given in eqs (22a) and (23), which in turn was derived from eq (12)), which is a relation between the uncorrected interior enthalpy field and the time-dependence of the surface enthalpy, which is unaffected by the correction because the boundary condition stated in eq (8a) continues to be valid. Thus the H that appears in all of the formulas of section 4 must continue to refer to the average value of the uncorrected interior enthalpy field, which means that the right way to make the desired correction is to substitute the right-hand side of

$$\dot{H} = \dot{H}_{\text{tot}} - \delta_\alpha\dot{H} \quad (59)$$

wherever $\dot{H}$ appears in a formula, and to identify $\dot{H}_{\text{tot}}$ with the observed heat flux.

The calorimetric formulas of section 4 yield $c(t)$ and $\alpha(t)$ as continuous functions of time from which $c(T)$ and $\alpha(T)$ are found. If, however, spline representations of $c(T)$ and $\alpha(T)$ are used, then the unknowns are the spline coefficients, which are constant numbers. Expressions for the coefficients as weighted integrals involving the observed functions $T(t)$ and $\dot{H}(t)$ could be derived from either the expansion or the integral forms of the calorimetric formulas. Because the spline coefficients are expressed as integrals of the observed data, there would be an automatic smoothing, which could be advantageous in the case of noisy data.

Although the calorimetric formulas derived in section 4 were intended to be used with observational data from a single observational run using a single sample, it would also be possible to use them with data from two different runs over the same temperature range using a large and a small sphere of the same material. The radius of the small sphere would be made small enough so that the observations would be in the extreme post transient regime $(T < \tfrac{1}{4})$ where the accuracy of eq (44) for c would be good. The functional dependence for $c(T)$ found in this way could then be substituted into the left-hand side of eq (41a), and data from the run with the larger sphere could be inserted into this equation, which would be solved for α. This two-sphere approach had been suggested by Colwell [1,2] when he first proposed radiometric calorimetry of freely cooling spheres.

Because the calorimetric formulas have been derived from an analysis that did not require a knowledge of the cooling law, but rather only the time-dependence of the

total rate of heat loss (or gain), they could be applied to any situation in which the interior temperature profile of a sphere is determined by the changing temperature of its external environment. For example, in the case of differential scanning calorimetry, using the calorimetric formulas would permit a determination of the thermal parameters of a spherical sample even when the time-rate of change of the surface temperature of the sample (i.e., the scanning rate) was so fast that the sample interior would be far from isothermal. This would permit a faster scanning rate, which would in turn cause larger heat fluxes which could be measured with greater precision than the small ones that result when the scanning rate is slow enough to keep the sample interior essentially isothermal. Moreover, the differential scanning technique would no longer be limited to the measurement of heat capacitance, but could also be used for measurements of thermal diffusivity.

Finally, because the analysis does not assume that the measured quantities are monotonic in time, it could be adapted to modulation calorimetry in which the sample surface is subjected to a periodically varying temperature and the magnitude and phase lag of the heat flux as a function of the frequency of the temperature variation are the measured quantities from which the thermal properties are deduced. Although the basic approach of this paper would still be applicable, it would be necessary to subject the surface-driven solution of section 2 to a Fourier analysis in order to express the various quantities as functions of frequency rather than of time.

---

6. References

[1] Colwell, J.H., NBS: Properties of Electronic Materials, NBSIR 79-1761, J.R. Manning, ed., (National Bureau of Standards, 1979). Cf. pp. 103-131.

[2] Colwell, J.H., NBS: Materials Measurements, NBSIR 80-2080, J.R. Manning, ed., (National Bureau of Standards, 1980). Cf. pp. 83-113.

[3] Carslaw, H.S.; Jaeger, J.C., Conduction of Heat in Solids, (Oxford University Press, New York, 2nd ed., 1959).

[4] Özişik, M.N., Heat Conduction, (John Wiley & Sons, New York, 1980).

[5] Jones, B.F., The Determination of a Coefficient in a Parabolic Differential Equation Part I. Existence and Uniqueness, J. Math. Mech. 11, 907-918 (1962).

[6] Douglas, J.; Jones, B.F., The Determination of a Coefficient in a Parabolic Differential Equation Part II. Numerical Approximation, J. Math. Mech. 11, 919-926 (1962).

[7] Jones, B.F., Various Methods for Finding Unknown Coefficients in Parabolic Differential Equations, Comm. Pure Appl. Math. 16, 33-44 (1963).

[8] Cannon, J.R.; Jones, B.F., Determination of the Diffusivity of an Anisotropic Medium, Int. J. Eng. Sci. 1, 457-460 (1963).

[9] Cannon, J.R., Determination of Certain Parameters in Heat Conduction Problems, J. Math. Anal. Appl. 8, 188-204 (1964).

[10] Cannon, J.R.; DuChateau, P.C.; Filmer, D.L., A Method of Determining Unknown Rate Constants in a Chemical Reaction in the Presence of Diffusion, Math. Biosciences 9, 61-70 (1970).

[11] Cannon, J.R.; DuChateau, P.C., Determining Unknown Coefficients in a Nonlinear Heat Conduction Problem, SIAM J. Appl. Math. 24, 298-314 (1973).

[12] Cannon, J.R.; DuChateau, P.C., Determination of Unknown Physical Properties in Heat Conduction Problems, Int. J. Eng. Sci. 11, 783-794 (1973).

[13] Cannon, J.R.; DuChateau, P.C., An Inverse Problem for a Nonlinear Heat Equation, SIAM J. Appl. Math. 39, 272-289 (1980).

[14] Abramowitz, M.; Stegun, I.A., eds., Handbook of Mathematical Functions, Natl. Bur. Stand. (U.S.) Appl. Math. Ser. 55 (1964).

[15] Magnus, W.; Oberhettinger, F.; Soni, R.P., Formulas and Theorems for the Special Functions of Mathematical Physics, (Springer-Verlag, New York, 1966).

[16] Chambré, P.L., Nonlinear Heat Transfer Problem, J. Appl. Phys. 30, 1683-1688 (1959).

INDEX TO VOLUME 87

January-December 1982